FLORIDA INTERNATIONAL UNIVERSITY

Miami, Florida

INVESTIGATION OF MOLECULAR MECHANISMS OF LKB1 FUNCTION IN *DICTYOSTELIUM* DEVELOPMENT AND STRESS RESPONSES AND THE FUNCTION OF SUPEROXIDE DISMUTASE C (SODC) IN CHEMOTAXIS

A dissertation submitted in partial fulfillment of the

requirements for the degree of

DOCTOR OF PHILOSOPHY

in

BIOLOGY

by

Sudhakar Veeranki

2009

To: Dean Kenneth Furton
College of Arts and Sciences

This dissertation, written by Sudhakar Veeranki, and entitled Investigation of Molecular Mechanisms of LKB1 Function in *Dictyostelium* Development and Stress Responses and the Function of Superoxide Dismutase C (SodC) in Chemotaxis, having been approved in respect to style and intellectual content, is referred to you for judgment.

We have read this dissertation and recommend that it be approved.

Alejandro Barbieri

Fenfei Leng

John Makemson

Lidia Kos

Leung Kim, Major Professor

Date of Defense: May 11, 2009

The dissertation of Sudhakar Veeranki is approved.

Dean Kenneth Furton
College of Arts and Sciences

Dean George Walker
University Graduate School

Florida International University, 2009

DEDICATION

I dedicate this dissertation to my parents and sister.

ACKNOWLEDGMENTS

With the deepest gratitude, I would like to acknowledge all the persons behind completion of this dissertation. First and foremost I would like to thank my major professor Dr. Leung Kim, for guiding me through all the difficult tasks of dissertation and my committee members: Alejandro Barbieri, Lidia Kos, John Makemson, and Fenfei Leng for their teaching, guidance, and constructive criticism throughout the years. I am grateful for my fantastic colleagues in the lab for their support, especially, Bohye Kim, Dr. Namshik Lee, Marbelys Rodriguez, and Osmin Anis who helped me with my projects at various levels. Special thanks to Osmin Anis for his affable companionship through-out my dissertation work. Additionally, I would like to recognize Sun Tong, for his help during teaching. I duely acknowledge the cordial permission from the 'Journal of Cell Science' for allowing me to use the copyrighted article (Veeranki et al., 2008) to adapt and/or modify towards my dissertation (Chapter 2). I greatly appreciate the financial support of the FIU graduate school for supporting me through Presidential and Dissertation year fellowships. I am grateful to my friends and colleagues, for their help and companionship.

ABSTRACT OF THE DISSERTATION

INVESTIGATION OF MOLECULAR MECHANISMS OF LKB1 FUNCTION IN *DICTYOSTELIUM* DEVELOPMENT AND STRESS RESPONSES AND THE FUNCTION OF SUPEROXIDE DISMUTASE C (SODC) IN CHEMOTAXIS

by

Sudhakar Veeranki

Florida International University, 2009

Miami, Florida

Professor Leung Kim, Major Professor

The serine/threonine kinase LKB1 is a regulator of critical events including development and stress responses in metazoans. The current study was undertaken to determine the function of LKB1 in *Dictyostelium*. During multicellular development and in response to stress insult, an apparent increase in the DdLKB1 kinase activity was observed. Depletion of DdLKB1 with a knockdown construct led to aberrant development; a severe reduction in prespore cell differentiation and a precocious induction of prestalk cells, which were reminiscent of cells lacking GSK3, a well known cell-fate switch. Furthermore, *DdLKB1* depleted cells displayed lower GSK3 activity than wild type cells in response to cAMP stimulation during development and failed to activate AMPK, a well known LKB1 target in mammals, in response to cAMP and stress insults. These results suggest that DdLKB1 positively regulates both GSK3 and AMPK during Dictyostelium development, and DdLKB1 is necessary for AMPK activation during stress response regulation. No apparent GSK3 activation was observed in response to stress insults.

Spatial and temporal regulation of phosphatidylinositol-(3,4,5)-triphosphate (PIP3) along the membrane of polarized cells is important for efficient chemotaxis. A REMI screen for PIP3 suppressors in the absence of stimulation led to the identification of SodC as PIP3 regulator. Consistent with their higher PIP3 levels, *sodC*$^-$ cells showed defects in chemotaxis and exhibited higher intra-cellular superoxide levels. Protein localization studies along with observations from GPI specific PI-PLC treatment of wild-type cells suggested that SodC is a GPI anchored outer-membrane protein. SodC showed superoxide dismutase activity in vitro, and motility defects of *sodC*$^-$ cells can be rescued by expressing the intact SodC but not by the mutant SodC, which has point mutations that affect its dismutase function. Treatment of *sodC*$^-$ cells with LY294002, a pharmacological inhibitor of PI3K, partially rescued the polarization and chemoattractant sensing defects but not motility defects. Consistent with increased intracellular superoxide levels, *sodC*$^-$ cells also exhibited higher basal Ras activity, an upstream regulator of PI3K, which can be suppressed by a cell permeable superoxide scavenger, XTT, indicating that SodC is important in regulation of intracellular superoxide levels thereby regulating the Ras activity and PIP3 levels at the membrane.

TABLE OF CONTENTS

LIST OF FIGURES

LIST OF ABBREVIATIONS

TERM/UNIT OF MEASUREMENT	SYMBOL/ABBREVIATOPNS
N-2-Hydroxyethylpiperazine-N'-2-ethanesulfonic acid	HEPES
4-hydroxy-2-*trans*-nonenal	HNE
4-[3-(4-iodophenyl)-2-(4-nitrophenyl)-2*H*-5-tetrazolio]-1,3-benzene disulfonate	WST-1
5-bromo-4-chloro-3-indolyl-β-D-galactopyranoside	X-gal
Adenosine monophosphate	AMP
Adenosine triphosphate	ATP
Alanine	A
AMP activated kinase	AMPK
Atypical protein kinase C	aPKC
cAMP activated receptors	cARs
Complementary DNA	cDNA
Conditioned medium	CM
Curie	Ci
Cyclic 3',5' adenosine mono phosphate	cAMP
Cyclic 3',5' guanosine mono phosphate	cGMP
Cytosolic regulator of Adenylyl cyclase	CRAC
Degree Celsius	^{o}C
Deoxyribose nucleic acid	DNA
Dictyostelium discoideum LKB1	DdLKB1
Differentiation inducing factor-1	DIF-1

Epidermal growth factor	EGF
Filamentous actin	F-actin
Globular actin	G-actin
Glycogen synthase kinase 3β	GSK3β
Glutamate	E
G protein coupled receptors	GPCR
Gram	g
Green fluorescent protein	GFP
Guanosine diphosphate	GDP
Guanosine triphosphate	GTP
Hour	hr
Hydrogen peroxide	H_2O_2
Immunoblot	IB
Immunoprecipitation	IP
Liter	l
Lymphoid enhancer factor 1	Lef1
Mega base pairs	Mb
Microgram	µg
Microliter	µl
Micrometer	µm
Micromolar	µM
Micron	µ
Milligram	mg

Milliliter	ml
Millimeter	mm
Millimolar	mM
Minutes	min
Mouse protein 25	MO25
Myelin basic protein	MBP
Nanogram	ng
Nanometer	nm
Nanomolar	nM
Nitro blue tetrasolium salt	NBT
Nonyl phenoxylpolyethoxylethanol	NP-40
Percent	%
p90 ribosomal S6 protein kinase	RSK
Phosphatase and tensin homolog	PTEN
Phosphoinositol 3 kinase	PI3K
Phosphoinositol tri (3,4,5) phosphate	PIP3
Piperazine-1,4-bis[2-ethanesulfonic acid]	PIPES
Pleckstrin homology	PH
Polymerase chain reaction	PCR
Protein kinase A	PKA
Protein kinase B	PKB
Protein tyrosine phosphatase	PTP
Ras binding domain	RBD

Reactive oxygen species	ROS
Restriction enzyme mediated integration	REMI
Reverse transcription PCR	RT-PCR
Ribonucleic acid	RNA
Ribosomal RNA	rRNA
RNA interference	RNAi
Serine	S
Signal transducer and activator of transcription	STAT
Sodium fluoride	NaF
STE20 related adaptor	STRAD
Superoxide radical	O_2^-
Superoxide dismutase	SOD
T-cell factor 1	Tcf1
Tetrazolium dye sodium,3′-(1-[phenylamino-carbonyl]-3,4-tetrazolium) -bis(4-methoxy-6-nitro) benzene-sulfonic acid hydrate	XTT
Ultraviolet	UV
Water	H_2O
Wild type	Wt
Zaphod kinase	ZAK

Chapter 1

Introduction

1.1 *Dictyostelium* a model organism

Dictyostelium discoideum is a single cell amoeba. They undergo multicellular development when the cells are deprived of food. In response to depletion of food in their environment, the amoebae start secreting 3'-5'-cyclic adenosine monophosphate (cAMP) which is a morphogen and also a chemoattractant. In response to cAMP, cAMP receptors (cARs), members of G protein coupled receptor (GPCR) family, initiate signaling events that translate cAMP gradient into directional movement. About a million of amoebae chemotaxis towards a cAMP center and form a compact structure called a mound. Cell differentiation and cell sorting within the mound results in an elongated structure called a slug, with prestalk-cell-enriched front and prespore-cell-dominating back. When the slugs find the right environment, these prestalk and prespore cells commit a terminal differentiation and form a final culminating structure known as 'fruiting body'. The fruiting bodies have a spore cup upheld by a single stalk. Spores, from the spore cups, are released into the surroundings, germinate and start their individual lives by preying on bacteria (Chisholm and Firtel, 2004).

Dictyostelium has been studied as a model organism for dissecting signaling networks involved in multicellular development, stress mediated responses and chemotaxis. Some of the features that make *Dictyostelium* a model organism are: it has simple and defined nutritional requirements; it is easy to maintain in the lab; its haploid genome enables the elegant genetic screens; its completely sequenced genome (34Mb) has a modest number of genes (~8000-10,000) yet maintains the complexity of signal regulatory networks comparable to higher multicellular organisms; it is capable of performing chemotaxis mediated aggregation dependent transition from single cell to

multicellular development; it can be synchronized *in vitro* by cAMP pulsing for acquiring chemotactic and developmental competence; and finally, it has a developmental life cycle that lasts for ~24 hrs with two kinds of differentiated cells undergoing morphogenetic movements analogous to higher multicellular organisms (Chisholm and Firtel, 2004).

1.2 Developmental signaling

Dictyostelium development consists mainly of two cell types: prespore and prestalk cells. Cell differentiation is orchestrated by two morphogens, cAMP and differentiation inducing factor-1 (DIF-1), a chlorinated alkyl phenone. During early development cAMP stimulates prespore and prestalk cell differentiation, whereas DIF-1 facilitates prestalk differentiation. Stimulation of cell differentiation by cAMP is mediated by preferential expression of either cAR3 or cAR4 that augment prespore or prestalk pathways, respectively. The immediate downstream effectors under the activated cAR3 and cAR4 receptors responsible for cell fate specification are not characterized (Chisholm and Firtel, 2004). However, cAR3 activates tyrosine kinase ZAK1 and cAR4 activates a putative PTP (protein tyrosine phosphatase). Differential regulation of GSK3 Y214 phosphorylation, which induces the GSK3 kinase activity, by these two receptors, is important in cell fate determination. Upon activation, ZAK1 directly phosphorylates and up regulates GAK3 (glycogen synthase kinase 3) activity. GSK3 activity is important in the determination of the cell's fate, as up regulation of GSK3 activity by ZAK1 specifies the prespore pathway, whereas absence of GSK3 activity specifies the prestalk pathway (Ginsburg and Kimmel, 1997; Harwood et al., 1995; Kim et al., 2002; Kim et

al., 1999; Plyte et al., 1999). It will be of great significance to know the immediate upstream activator of ZAK1 in specification of prespore pathway.

Recent studies in vertebrate Wnt signaling showed that LKB1, a serine threonine kinase that when mutated causes Peutz-Jeghers syndrome in humans, is an upstream regulator of GSK3 during morphogenesis and cell fate determination. However, it is not clear if Wnt signal is modulating LKB1 activity (Ossipova et al., 2003). The current study is aimed to understand if extracellular signals, such as cAMP and stress, orchestrate the LKB1 and GSK3 using *Dictyostelium* as a model organism.

The *LKB1* homologues, *Par4* in *Caenorhabditis elegans* and *XEEK1* in *Xenopus*, perturb multiple developmental processes when they are mutated (Ossipova et al., 2003; Watts et al., 2000). Some of the developmental defects observed during the ablation of LKB1 activity in *Xenopus* embryos were the result of compromised Wnt signaling (Ossipova et al., 2003). It has been shown that synergistic activity of LKB1 on β-catenein stabilization with Wnt was the result of inhibition of GSK3β through aPKC (atypical protein kinase C), a kinase implicated in cell polarity of metazoans (Ossipova *et al*, 2003). Though the developmental defects observed in the absence of LKB1 in *Xenopus* embryos have some resemblance to Wnt activated transcription factor [Tcf1-Lef1 (partners for β-catenin in formation of transcription activation complex)] knockout organisms, there are also dissimilarities, suggesting additional effectors for LKB1 during development. Mice lacking LKB1 display complex phenotypes during embryogensis (Ylikorkala et al., 2001). The Mouse and *Xenopus* studies suggested the existence of multiple targets for LKB1 during development. *Dictyostelium* has a well conserved *LKB1* homologue: *DdLKB1* (Dictybase genome project); the function of DdLKB1 in

Dictyostelium has yet to be characterized. Given the potential for providing additional insights about how LKB1 regulates multicellular development, and how LKB1 interacts with other signal molecules in response to diverse stimuli, it will be of great use to characterize the role of LKB1 in *Dictyostelium* development.

Accumulated body of evidence has identified LKB1 as a multi-tasking master kinase with roles in metabolism, cell polarity, cell cycle control and development (Alessi et al., 2006; Marignani, 2005). These diverse roles are expected of LKB1, as it was shown that LKB1 phosphorylates and regulates 13 of the AMPK (AMP activated kinase) related family of protein kinases (Lizcano et al., 2004). Mammalian LKB1 was found to be associated in protein complexes in cells. The two partners for LKB1 are STE20 related adaptor (STRAD, a pseudo kinase) and MO25 (a scaffolding protein) (Baas et al., 2003; Boudeau et al., 2003; Boudeau et al., 2004). Recent studies showed that LKB1 is a constitutively active protein kinase and its kinase activity is further up-regulated ten-fold upon forming a protein complex with STRAD and MO25 (Boudeau et al., 2004; Alessi et al., 2006). Cytosolic localization of LKB1 is also regulated by STRAD. Phosphorylation at S431 of LKB1 was characterized, and mutations at this site (S431E and S431A) have been found to affect its ability to suppress cell growth. However, mutation that prevent phosphorylation (S431A) and mutation that mimic phosphorylation (S431E) have no effect on the LKB1 kinase activity or its localization, suggesting that such mutations might alter the ability of the LKB1 to form appropriate complexes (Fogarty and Hardie, 2009). Two upstream LKB1 kinases responsible for S431 phosphorylation were identified: Protein kinase A (PKA) and p90-kDa ribosomal S6 protein kinase (RSK). Convincing *in vivo* evidence has been presented for S431 phosphorylation by these kinases. Both

forskolin and a cell permeable cAMP analogue induce the S431 phosphorylation through PKA, whereas EGF induces S431 phosphorylation through p90 RSK in Rat cell lines. It has been postulated that PKA and RSK exibit their growth suppression effects through LKB1 (Sapkota et al., 2001). However, it is not well known how LKB1 exerts its effects.

1.3 Stress signaling

Dictyostelium also has been a model for studying stress related pathways. Typical stress responses involve cessation of growth and cell multiplication, cytoskeletal rearrangements and changes in cell shape, as well as induction of target genes which will govern long term adaptation. Previous studies have revealed many components involved in the regulation of stress responses in *Dictyostelium* especially with hyper-osmotic shock (Araki et al., 2003; Gamper et al., 1999; Ott et al., 2000; Oyama, 1996). Though many secondary messengers and signaling compounds have been identified as hyper-osmotic sensors, the complete signal cascade/flow regulating these stress responses is still elusive. Many of these compounds have direct homologues in higher eukaryotes [cAMP, cGMP, PKA, YakA (homologue of yeast dual specificity kinase Yak1p), and STAT (signal transducer and activator of transcription)]. Because, *Dictyostelium* shares many important signaling molecules with higher eukaryotes, including LKB1; the present study has made an attempt to further elaborate on the modulation of LKB1 in response to several types of stress in *Dictyostelium*.

Multiple studies using various mammalian cell lines showed that LKB1 activity is up regulated in response to oxidative (H_2O_2) and osmotic (sorbitol) stress, which further activates its downstream kinase AMPK, as observed by increased phospho AMPK levels

in a LKB1 kinase activity dependent manner (Qiu et al., 2006; Shaw et al., 2004; Woods et al., 2003). It was shown that oxidative stress can activate AMPK in a AMP/ATP independent and dependent manner (Choi et al., 2001; Takeda et al., 2007). Stress induced activation of AMPK was suggested to decrease catabolic pathways and increase anabolic pathways to restore the AMP/ATP ratios back to normal (~0.2). The above mentioned studies provided not only evidence for LKB1's role in mediating stress dependent responses, but also AMPK as its downstream mediator in such stress responses. However, it was not known how such stress stimulations result in LKB1 activation.

1.4 Chemotaxis signaling

Activation of cAR1 induces a cascade of events, including Ras activation, membrane localization of phosphoinositol-3- kinase (PI3K) and generation of phosphoinositol tri-(3,4,5)Phosphate (PIP3) at the membrane (Chisholm and Firtel, 2004). The two major PIP3 regulators PI3K and PTEN (Phosphatase and Tensin homolog) localize to the plasma membrane in a mutually exclusive manner that PIP3 accumulates at the front part of the polarized cells, facing the higher side of the cAMP gradient (Funamoto et al., 2002; Merlot and Firtel, 2003). Polarized accumulation of PIP3, in turn, leads to an asymmetric recruitment of PH (Pleckstrin homology) domain containing proteins to the front and stimulation of pseudopod extension.

The importance of spatial and temporal regulation of PIP3 levels at the membrane of polarized cells in proper polarization and directional motility was also confirmed further by studies with cells lacking PTEN. In the absence of PTEN, there was evidence

of prolonged and broadened PIP3 accumulation at the membrane as well as F-actin levels coincident with defective chemotaxis (Iijima and Devreotes, 2002). These studies used GFP-$PH_{\mathbf{crac}}$ (cytosolic regulator of Adynyl cyclase) protein recombinant protein for visualizing the PIP3 levels indirectly.

A previous study showed that Ras, specifically RasG, is selectively activated at the front parts of polarized cells, and activate PI3K at the front part of the polarized cell membrane (Sasaki et al., 2004). It was proposed that initial activation of Ras at the front will form a positive feedback loop involving PI3K and F-actin, which further intensifies the active Ras levels at the front and enables the cells to become polarized in gradients as narrow as a 2-5% difference between the front and back of the cell. However, it is not known how Ras was selectively activated at the membrane closest to the source of the chemoattractant. Moreover, it was also shown that Ras can be activated independently of Gβγ, activated G protein subunits (Sasaki et al., 2007), leaving the mechanism of Ras activation in *Dictyostelium* largely unknown.

The current study was undertaken to shed more light on the molecular mechanisms of chemotaxis in general, and specifically to identify the additional suppressors of PIP3 at the membrane in the absence of chemoattractant stimulation by using restriction enzyme mediated integration (REMI) strategy in wild type cells expressing PIP3 marker, GFP-PH_{CRAC}.

Chapter 2

INVESTIGATION OF MOLECULAR MECHANISMS OF LKB1 FUNCTION IN *DICTYOSTELIUM* DEVELOPMENT AND STRESS RESPONSES

2.1 Materials and methods

2.1.1 *Dictyostelium* development and growth

Axenic strains (AX3, and AX2) were grown axenically using D3T medium (7.15 g/l Bacto peptone #3, 7.15 g/l thiotone, 7.15m g/l yeast extract, 15.4 g/l glucose, 0.48 g/l KH_2PO_4, 0.525 g/l Na_2HPO_4) or on SM agar plates as described by Sussman, 1987. Auxotrophic strain JH10 (Ax3 derived auxotrophic strain) cells were grown in D3T supplemented with thymidine (0.5 mg/ml). Cells with selection markers were grown with D3T supplemented either with Neomycin (G418) (20 μg/ml to 80 μg/ml) or Blasticidin (5 μg/ml) as required. Log phase cells were used for transformation by electroporation. Log phase cells were washed with Development buffer (DB) and plated on nitrocellulose membranes at 25 million cells per membrane. For development in suspension culture, cells were starved for an hour in a flask with shaking, stimulated with 50 nM cAMP pulses at 6min interval for 4 hr, and were further stimulated with a final pulse of 300 μM cAMP.

2.1.2 RT-PCR

Total RNA was isolated at indicated time points using Trizol reagent (Invitrogen). The RNA concentrations were adjusted to 1 g/l in all time points according to spectrophotometric measurements and verified again by gel loading and spectrophotometry. One step RT-PCR reaction was performed by using C-Master RT PCR kit (Eppendorf) and 0.3μg of total RNA. *DdLKB1* was amplified by using primers forward (5'TACATCGTGATATTAAACCTG3') and reverse (5'CATCATCTTGACCA CTACTAGC3'). *Dictyostelium* Mitochondrial rRNA message (*IG7)* was used as an

internal control for RT-PCR reaction and was amplified using forward primer (5'GGTGAGCGAAAGCCGAGGAGAG3') and the reverse primer (5'GCAACA GTTACGGGTTCCGCC3'). For the prestalk marker *ecmA* amplification, the forward primer (5' CAGCCAAAGGTTGCATC GAAGTCCCAATGA 3') and the reverse primer (5' ACCTCCTGTACCACCAATGAGACCACC 3') were used. The *ecmB* was amplified using the forward primer (5' TGAATTGCGACGATGGTAACTTCTGTAC 3') and the reverse primer (5' TCCAA ATGTTTTGCATTGGGTCATTGGA 3'). *carA1*, *ampA1*, *dscA1*, and *dscD1* transcrits were amplified using the following forward and reverse primers: *carA1*forward (5' ATGGGTCTTTTAGATGGAAATCCAGCC 3') and reverse (5' CCAACCAATACTGCTGAAATTGCCC 3'); *ampA1*forward (5' GATTGCTCCCTC GTTAGATGTGCCC 3') and reverse (5' CAAAATCTTTGGACATGGAACTCTTG 3'); *dscA1*forward (5' CCCAAGGTTTAGTTCAACTCCTCGC 3') and reverse (5' CAGTG TTACGATCAGTTACACCAGTAAC 3'); and *dscD1* forward (5' CCCAAGGTTTA GTTACACTTCTCGG 3') and reverse (5' GTAGAATTCACATCTTAATGAAATGT GG 3').

2.1.3 DdLKB1 promoter cloning

The 1915 bp of the intergenic region upstream of *DdLKB1* (DDB0205947), before the next gene CYP513G1P (DDB0205948), was PCR amplified using primers Pro-LKB1F1 (5' GGATTTAGCTGCTTATGGAATTGGTG 3') and Pro-LKB1R1 (5' GTATATGATGGTTGTTGTTCAACTTCC 3'). The amplification adds *SpeI* and *BglII* sites for directional cloning. The PCR product was cloned into the PCR vector (invitrogen) and verified the sequence by sequencing. The pAct15-Gal (Harwood and

Drury, 1990) was digested with XbaI and BglII to liberate the Actin 15 promoter and to clone the LKB1 promoter to generate expression vector pLKB1-Gal.

2.1.4 X-gal staining

One million log phase cells expressing pLKB1-Gal were washed with DB buffer and plated onto nitrocellulose filters (47 mm) for development. The structures were fixed with 1% glutaraldehyde in Z-buffer (60 mM Na_2HPO_4, 40 mM NaH_2PO_4, 10 mM KCl, 1 mM $MgSO_4$) for 10 min, dried for 20 min in the hood, permeabilized with 1% NP-40 in Z-buffer for 20 min at room temperature, washed twice with Z-buffer, and stained overnight by submerging in X-gal solution (1 mM potassium ferrocyanide, 1 mM potassium ferricyanide, and 0.5 mg/ml X-gal in Z buffer). The staining was stopped by washing with Z-buffer (Powell-Coffman and Firtel, 1994). All the steps were done at room temperature.

2.1.5 Cloning of DdLKB1 cDNA

Complete DdLKB1 cDNA was reverse transcribed from AX3 RNA at 45^{o}C by One step RT PCR kit (Qiagen), run through Micropure EZ filter (Millipore) for enzyme removal, amplified by HotMaster-Taq DNA Polymerase (Eppendorf) using LKB1 F1 (5'-ATGGAAGTTGAACAACAACCATC-3') and LKB1R3 (5'-AAAACTTAATT AATGATACATTTTGAC-3') primers, and cloned to PCR2.1 vector. The cDNA clone, pTOPO-LKB1, was verified by Big dye sequencing. The change from S128L is attributed to polymorphism and left intact.

2.1.6 Generation of T7-DdLKB1

The plamid, pTopo-LKB1 was used to generate T7 (MASMTGGQQMG)-DdLKB1. After sequence confirmation DdLKB1 was cloned in-frame into pCFC5 vector (Chen and Katz, 1998) downstream from T7 tag using *EcoRI* restriction site. To clone T7-LKB1 under SP60/Cotc promoter SL-25 vector was linearized with restriction enzymes SpeI and KpnI and insert was obtained by BglII and XhoI digestion from pCFC5. Both vector and insert were treated with Klenow enzyme for 15 min at 25^{o}C and were purified by ethanol precipitation before ligation.

2.1.7 Antibodies, western, and immuno-precipitation (IP)

Rabbit T7 (MASMTGGQQMG) affinity purified (QED Biosciences Inc.) antibody (1μg/μl) was used to detect T7-tag. Unless otherwise indicated 20 million cells were lysed at appropriate time points with 1ml of TTG buffer (TTG: 20 mM TrisCl (pH7.7), 1% Triton X-100, 5% Glycerol, 0.15 M NaCl, 1 mM EDTA, 1 mM Sodium vanadate, 40 μM ammonium molybdate) with protease inhibitors cocktail (Roche Inc). Antiboides against phospho-AMPK, Pan-Ras, GSK3 and phospho-GSK3 were purchased from Cell Signaling, Calbiochem, and Upstate Biotech.

2.1.8 DdLKB1 kinase assay

Log phase cells were lysed at appropriate time points and were immuno-precipitated by using 50 μl of Protein A Sepharose and 10 μl of T7 antisera for one and a half hours at 4^{o}C. After immunoprecipitation, the immunocomplexes were washed twice with TTG buffer and two more times with freshly made kinase buffer [20 mM TrisCl (pH

7.7), and 10 mM $MgCl_2$] at 4°C. Washed immunocomplexes were then incubated at 30°C for 20 min with 5μM ATP, 10 μCi of γ^{32}P-ATP, 10μg of Myelin Basic Protein (MBP), 20 mM TrisCl (pH 7.7), and 10 mM $MgCl_2$. The mixture was resolved by SDS-PAGE and autoradiagraphed on X-ray film.

2.1.9 RNAi strategy

Two PCR products were amplified using primers T-FI (5'CGCC GGAGATCTATGGAAGTTGAACAACAACCATC3'), T-R1 (5'CGCGGAAGCTTC AATTGGGTGCACTGGTAAACC3') and T-R2 (5'CGCCGGAAGCTTCTTTATCGA GATCATTTG GAAATTC3') and pTOPO-LKB1. The two reverse primers carry *HindIII* and the forward primer carries *BglII*. The PCR products were cloned into TOPO vector (Invitrogen) and were ligated back to back with *HindIII* so that the ligated product carries *BglII* at it ends. The final ligation product was digested with *EcoRI* and cloned into pCFC5 vector under Actin 15 promoter and confirmed by sequencing.

2.1.10 Northern hybridizations:

The total RNA was isolated using Trizol reagent and checked for integrity and used 10μg for assaying different probes on northern blots. IG7 was used for loading control. LKB1 probe was prepared by using primers F1 (5'ATGGAAGTTGAACAA CAACCATC3') and R8 (5'CAATTGGGTGCACTGGTAAACC3'). Labeling was done by Rediprime kit (Amersham).

2.1.11 Submerged aggregation assay

Log phase cells were plated at a density of $2.5x10^5$ cells per cm^2 in the DB buffer and incubated for 12 hr at 20^oC.

2.1.12 GSK3 kinase assay

Assay for GSK3 Kinase activity was done by following the method mentioned by Plyte et al., 1999. Cells were lysed in GS-lysis buffer (0.5% NP40, 10 mM NaCl, 20 mM PIPES, pH 7.0, 5 mM EDTA, 50 mM NaF, 0.1 mM Na_3VO_4 , 0.05% 2-mercaptoehanol) and supernatant was collected after centrifugation at 10,000 g at 4^oC for 10 minutes. After normalization for the total GSK3, each sample was incubated with peptide substrate (20μg of final concentration) and was assayed for 8 min in assay buffer (50 mM HEPES, pH 7.5, 4 mM $MgCl_2$, 0.5 mM EDTA, 2 mM DTT, 100 μM ATP, ~1000 cts/min per pmole [γ-^{32}P] ATP) of 20. μl. Assay was stopped by adding equal volume of 15 mM phosphoric acid. In parallel another sample was assayed in the presence of GSK3 inhibitor LiCl, to estimate the nonspecific background kinase activity levels. All samples were washed extensively in 7.5 mM phosphoric acid before taking scintillation counts. Assay was done three times with three independent samples.

2.1.13 Stress treatment:

Log phase cells were washed with DB buffer and were treated with either 2 mM H_2O_2 for 15 minutes or 200 mM sorbitol for 10 minutes as indicated in each experiment.

2.2 Results

2.2.1 Cloning and structural characterization of DdLKB1

Dictyostelium homologue (DdLKB1: DDB0229349) of human LKB1 was identified by searching in the Dictybase database. *DdLkb1* is of 1761 bp length and the protein size is 66.3 kd. DdLKB1 kinase domain (260 aa) has showed 40% identity to that of the human LKB1. As expected from a highly AT rich genome such as *Dictyostelium*, the c-terminal part of the LKB1 has homo-polymeric tracts which are responsible for the less homology of *Dictyostelium* LKB1 with the LKB1 of other species. As observed with the *Caenorhabditis elegans* and *Drosophila* the amino and carboxy terminal of the DdLKB1 are not conserved well when compared with human LKB1. Unlike human LKB1, DdLKB1 apparently lacks nuclear localization signal at its N-terminus. Farnesylation signal sequence at C-terminal is CIIN instead of typical CLIQ signal. Out of the four known autophosphorylation sites for human LKB1 (Alessi et al. 2006), DdLKB1 has only one conserved autophosphorylation site (T177). DdLKB1 has one putative consensus phosphorylation site for PKA at the C-terminus (at aa 534) which is also conserved in other species and one for PKB at the N-terminus (at aa 33) (Fig.2.1A). *Dictyostelium* also has homologues of human STRAD and MO25. The genes DDB0229911 and DDB0230012 share 46% and 45% homology with STARDα and STRADβ and DDB0218587 share 74% homology with MO25.

2.2.2 Spatial and temporal expression of DdLKB1

To determine the temporal expression pattern of LKB1 total RNA was isolated during the vegetative stage and during development of *Dictyostelium* at 5 hr intervals and was

checked for integrity. Limiting amounts of total RNA that was necessary for LKB1 amplification was determined by serial dilutions and it was 300 ng per reaction. Each reaction was accompanied by a positive control for IG7 amplification. Based on the ability to produce the LKB1 product from total RNA in a RT-PCR reaction, it seems that LKB1 is expressed in all stages as shown in Fig.2.1B. Relatively less expression was observed at the 5 hr developmental stage.

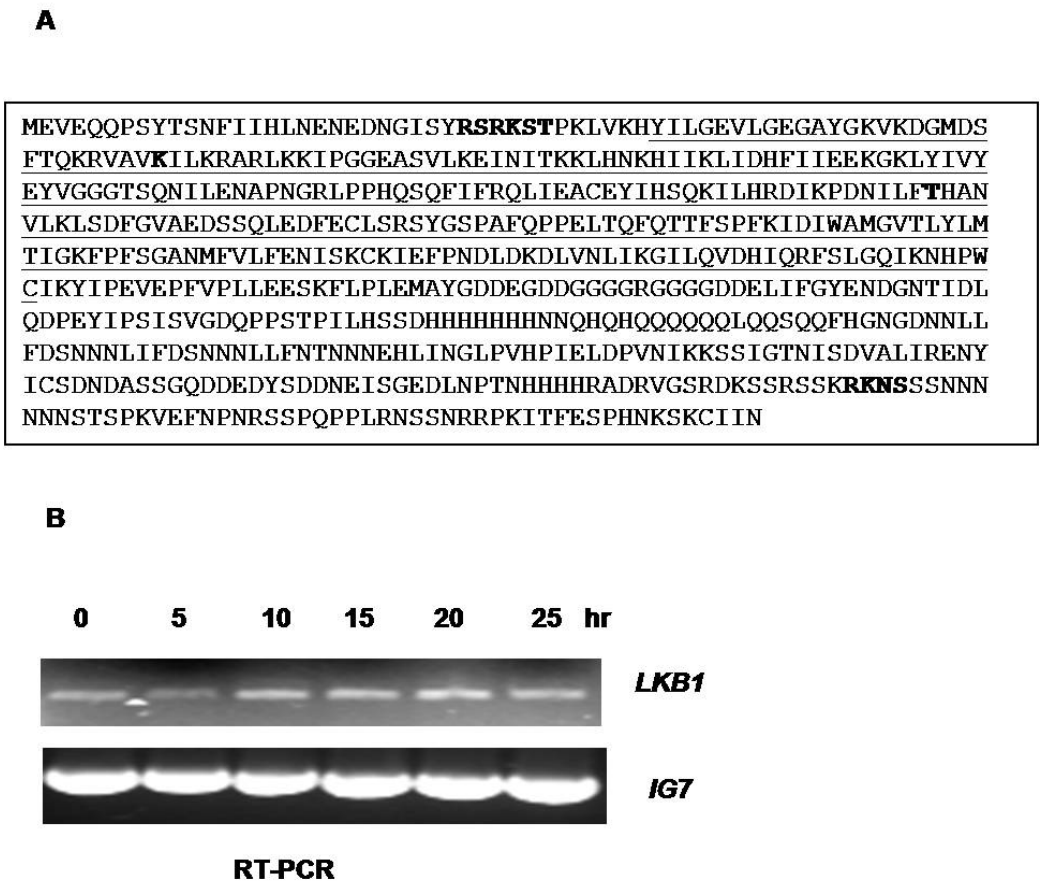

Figure 2.1 DdLKB1 sequence analysis and temporal expression pattern. **A.** Human homologue of *Dictyostelium* LKB1 (DdLKB1) amino acid sequence was shown. Kinase domain was underlined. Putative PKB and PKA consensus substrate phosphorylation sites were in bold. Also the only conserved autophosphorylation site T177 was shown in

bold. **B.** Expression of LKB1 at various developmental time points were revealed by RT-PCR with limiting amounts of total RNA. IG7 was also amplified by the same amount of total RNA to show the differences in LKB1 transcript levels at various developmental stages.

To test whether LKB1 is expressed ubiquitously in all cell types during multi-cellular development we chose to characterize the LKB1 promoter. Based on the genomic sequencing information provided by Dictybase, it was found that the inter-genic region between the first codon of LKB1 and its upstream gene (DDB0237445) is of 1715 bp in length. Additional 199 bases of 3' coding region of LKB1 upstream gene along with 1715 bp sequence was also included to ensure the integrity of the promoter was left intact. We cloned this inter genic region of 1915 bp (Appendix) upstream of *Lac Z* and developed the transformed *Dictyostelium* cells on nitrocellulose membrane and assayed for *β-Galactosidase* activity in the presence of X-gal. As shown in Fig.2.2, at 12hr the expression was seen all over the tight mound except at its tip where it was less intensely stained. The expression was later on restricted to the posterior 80% of the slug and to the spore bearing cup in terminally differentiated structure except at the anterior tip. This pattern of expression was highly analogous to prespore specific gene expression as described for PSPB, CotC, CotB, and CotA proteins (Fosnaugh and Loomis, 1993; Powell-Coffman and Firtel, 1994). Further analysis of *Ddlkb1* promoter has revealed that *lkb1* promoter has 4 typical CA rich elements (CAEs) that would be necessary to confer pre-spore specific expression (Powell-Coffman et al., 1994). Moreover two of these elements are (Appendix) situated with a typical spacing that was showed to bind to nuclear proteins such as GBF (G-box binding factor).

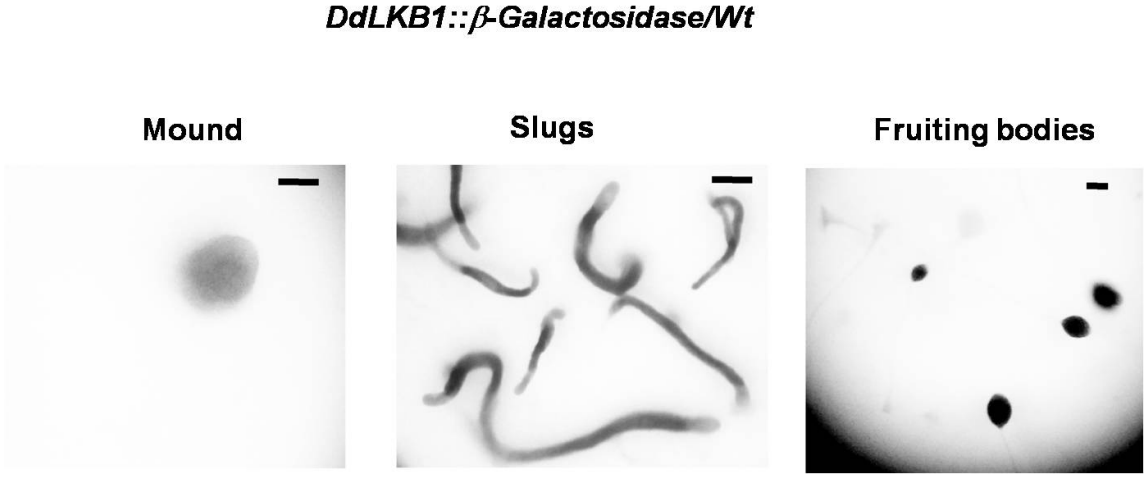

Figure 2.2 DdLKB1 spatial expression pattern. Expression of LKB1 message in different cell types during development as revealed by staining for the *β-Galactosidase* activity after expressing the *β-Galactosidase* under putative LKB1 promoter. From left tipped mound (12 hrs), slugs (20 hrs), and fruiting bodies (25 hrs). Scale bars in mounds and slugs are 100 μm and that in fruiting body is 50 μm.

2.2.3 DdLKB1 has functional kinase activity

To know whether the DdLKB1 has functional kinase activity analogous to other homologues in other species, T7-tagged DdLKB1 (T7-DdLKB1) was generated and expressed in wild type background under actin 15 promoter. T7-DdLKB1 was immunopurified and assayed for kinase activity. As shown in Fig.2.3, T7-DdLKB1 exhibited the ability to phosphorylate myelin basic protein (MBP) as well as to autophosphorylate itself. These results suggest that DdLKB1 has a functional kinase activity as suggested by the sequence analysis.

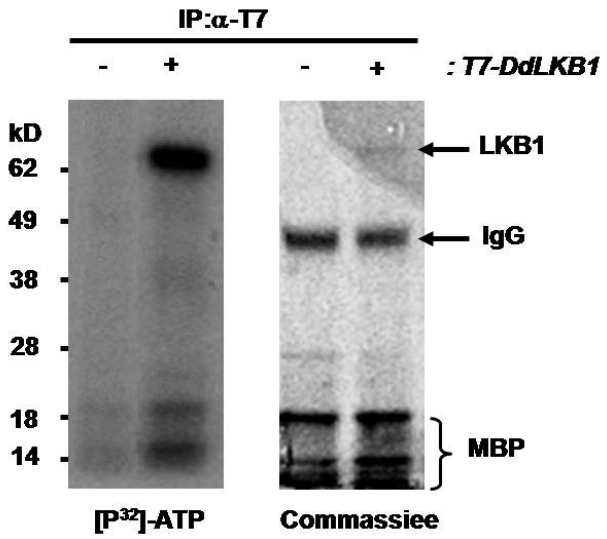

Figure 2.3 T7-DdLKB1 kinase assay. MBP was used as substrate. Cell lysate from wild type cells expressing T7-DdLKB1 was immunoprecipitated using T7 antiserum. Left autoradiogram and right coommassiee stained gel.

2.2.4 DdLKB1 activity is up regulated during development

To understand the role of LKB1 in the context of multicellularity, we decided to estimate the LKB1 activity at 5hr intervals from vegetative stage to terminal development. For this purpose we cloned the complete coding sequence of LKB1 with T7 tag under Actin 15 and also under the CotC promoter (prespore specific) to maintain the LKB1 expression till the terminal development. Log phase cells were developed on the nitrocellulose membranes and cell lysates were prepared at indicated time points. LKB1 protein is normalized first by western and then proceeded for the immunoprecipitation with limiting amounts of T7 antiserum and protein A and with excess amount of cell lysate. Kinase assay was performed using MBP as substrate as mentioned in the

methods. Though LKB1 is active in all stages tested including vegetative stage, LKB1 is relatively more active at 15, 20 and 25 hrs time points (Fig.2.4). At these stages two fold differences were seen when compared to the vegetative stage. These are the time points at which typical cell differentiation events take place. Starting with tight mound formation at ~15 hrs development cells start to differentiate into prespore and prestalk cells. The stages after 15 hrs development LKB1 activity varies but stays higher than the earlier stages. The greater variation at later stages of development could be due to time differences in culmination.

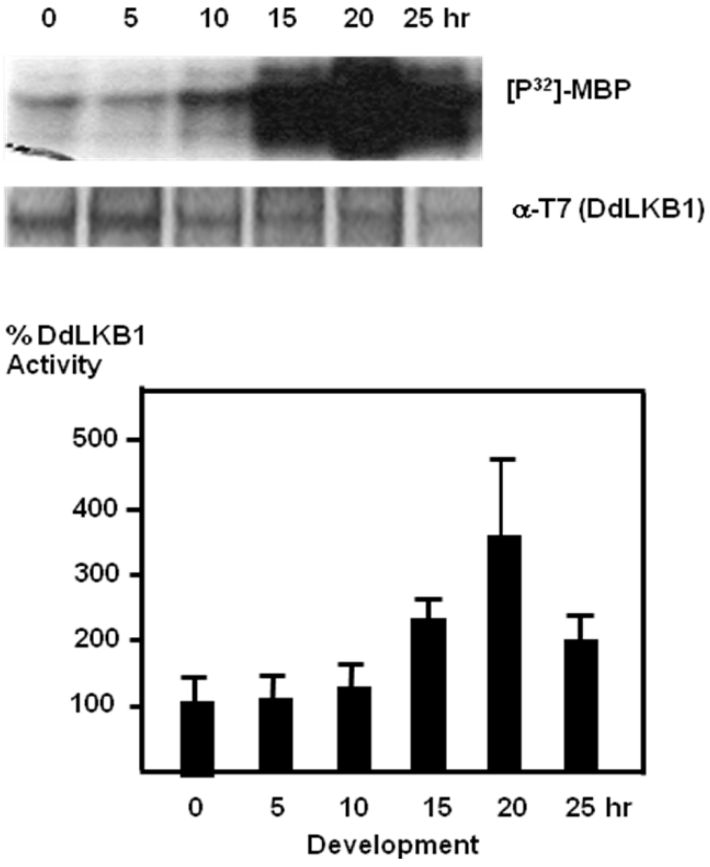

Figure 2.4 DdLKB1 kinase activity at various time points during *Dictyostelium* development. A representative western blot showing normalization of LKB1 proteins

used for kinase assay using anti-T7 anti serum and an autoradiogram showing the MBP phosphorylation by LKB1. Relative kinase activities from three different kinase assays were used to calculate average values with error bars and were shown at all developmental time points tested.

2.2.5 DdLKB1 activity can be modulated by morphogens cAMP and DIF-1

Cell fate decisions in *Dictyostelium* are regulated by external morphogens such as cAMP and DIF. Prespore differentiation is mediated by cAMP through cAR3 which belongs to seven trans-membrane receptor family. Because LKB1 kinase activity is up regulated during development, changes in LKB1 activity in response to cAMP and DIF stimulation were observed. Wild type cells over expressing the T7-LKB1 were synchronously developed for 5 hrs and then washed and stimulated with high cAMP (300 μM) or DIF-1 (200 nM) and cell lysates were prepared at indicated time points. As shown in Fig. 2.5A LKB1 kinase activity is up-regulated after 45 min of cAMP stimulation. After 60 min of cAMP stimulation there is a ~50% increase in the DdLKB1 kinase activity (Fig. 2.5A) which is however much less than the ~200% increase in the DdLKB1 activity (Fig. 2.4) observed during development. These results may suggest that DdLKB1 may function in response to external stimulants in a receptor dependent manner and in transducing external signals to determine cell fate specification. However, another membrane permeable morphogen DIF-1 also increased the LKB1 activity (Fig. 2.5B), though modestly (~30%), after an one hour suggesting receptor independent LKB1 activation during development. These results suggest that potentially different mechanisms may exist in regulation of LKB1 activity during development.

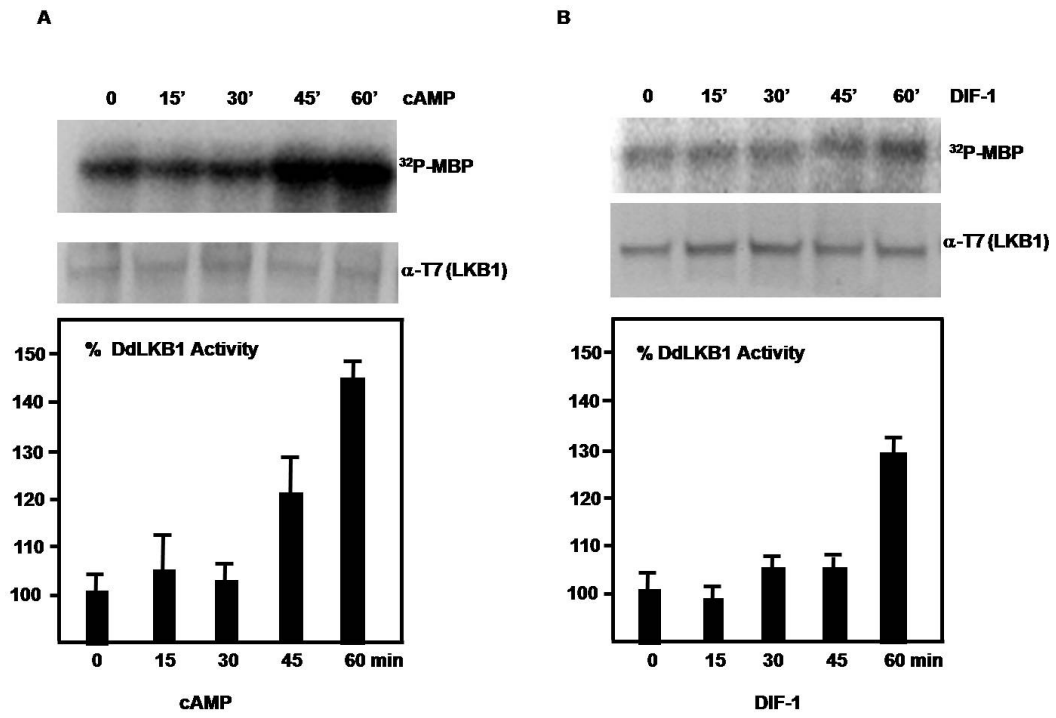

Figure 2.5 DdLKB1 kinase activity in response to morphogen stimulation. Amount of DdLKB1 kinase activity after stimulating with cAMP **(A)** or DIF-1 **(B)** were calculated from three independent experiments from developmentally competent cells and were shown with error bars. A representative western blot showing DdLKB1 levels used for kinase assay and a representative autoradiogram depicting the phophorylated MBP levels after kinase assay were shown for each of the stimulants at various time points indicated.

2.2.6 DdLKB1 regulates prespore gene expression

Presumptive prespore specific expression pattern of DdLKB1 and up regulation of DdLKB1 kinase activity suggested a possible role for DdLKB1 during development. To dissect this role further we sought to produce knock-out strains. But even after repeated attempts to make the LKB1 knock-out, I was unable to isolate LKB1 knock-outs. An

alternative track is to produce LKB1 knockdowns. RNAi was established in *Dictyostelium* to generate knockdowns of genes and especially useful for chromosomal regions with low recombination potential (Martens et al., 2002). Martens et al. has shown that stem loop structures are the efficient way of producing the knockdown (RANi) effect for a given gene in *Dictyostelium*. We transcribed the DdLKB1 using the Actin 15 promoter as inverted repeats separated by a loop as shown in Fig. 2.6. The inverted repeats span the first 817 bases of DdLKB1 and the loop region (500 bp) spans 813 bp-1363 bp of DdLKB1. We confirmed the knock down effect of DdLKB1 by northern hybridization (Fig. 2.7A). IG7 was used as the positive loading control. The DdLKB1 transcripts were reduced to 30% level. However, the empty vector at the same selection pressure did not produce any effect on DdLKB1 transcript.

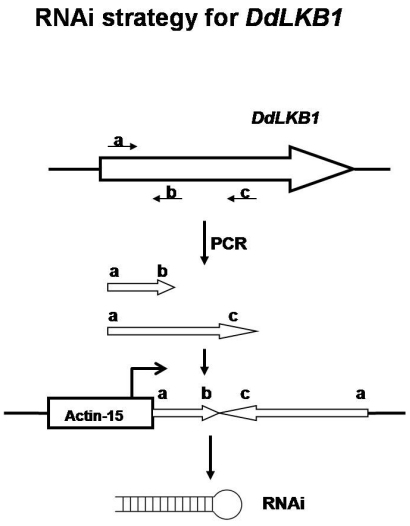

Figure 2.6 *DdLKB1* knockdown/RNAi strategy. Dd-LKB1 was amplified with primers a, b, and a, c and their relative positions were shown. ab and ac amplicons were ligated tail to tail to generate RNAi construct and was expressed under actin 15 promoter.

As described in the methods, log phase wild type and *DdLKB1* knockdown cells were plated on DB agar plates. As shown in Fig. 2.7B wild type cells could form slugs normally. However, knockdown cells were slow in aggregation and the size of the cell aggregate was drastically reduced. Though equal number of cells was plated, the size of aggregates was severely reduced in knockdown cells in comparison with wild type cells. Moreover, there was delay in formation of slugs. At 20 hrs development the *DdLKB1* knockdown did not form any slugs. Unlike wild type cells, knockdown cells did not form typical culmination structures even after 25 hrs of development. Though, knockdown cells could form typical culmination structures after 48 hrs of development, the size was drastically reduced and also *DdLKB1* knockdown cells displayed only ~20% of the spores compared to wild type cells (Fig. 2.8B). However, knockdown cells could form normal spores as spores from these cells were able to germinate properly. The severe nature of developmental defects observed in knock down cells suggests that DdLKB1 has a crucial role in cell differentiation process during multicellular development.

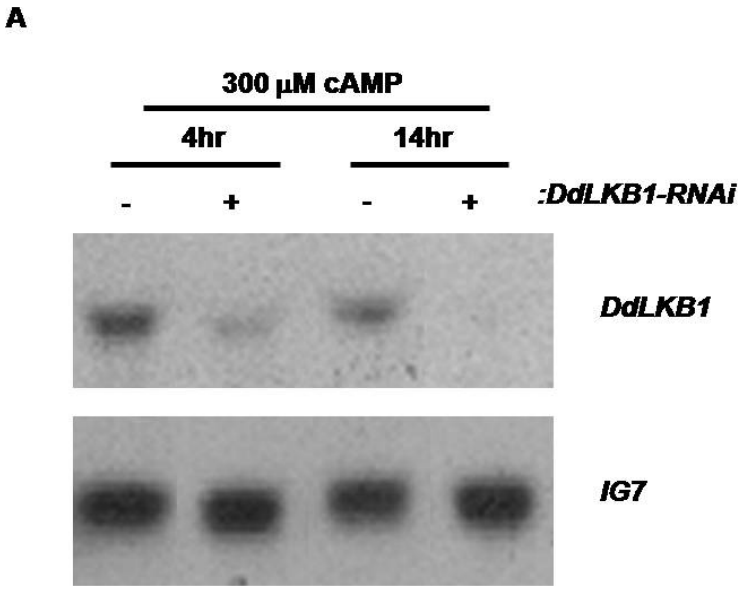

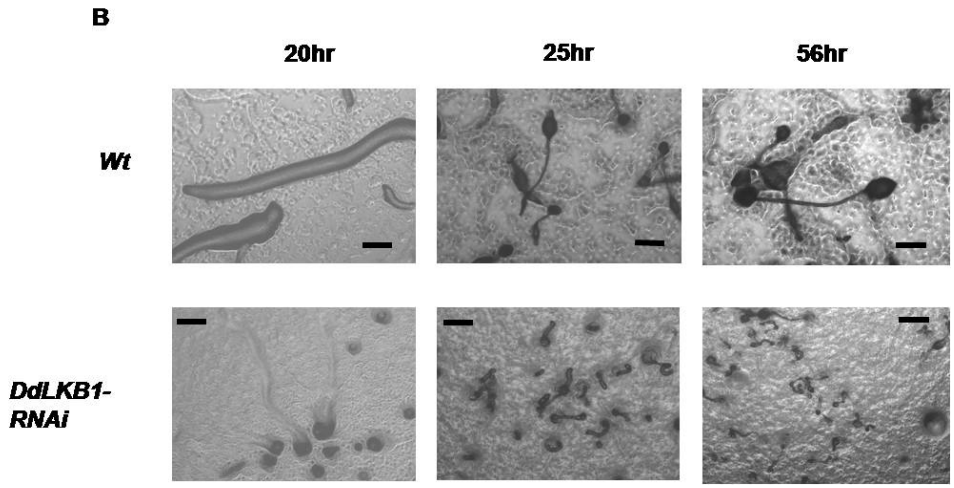

Figure 2.7 *DdLKB1* knockdown confirmation and its phenotype during *Dictyostelium* development. **A.** Northern blot showing LKB1 transcripts during synchronous development of wild type and *DdLKB1* knockdown cells. *IG7* was assayed as a loading control along with *DdLKB1*. **B.** Development on DB agar plates at different time points. All micrographs were taken at 10X magnification.

Knockdown cells were assayed for developmental prespore specific markers after developing them synchronously by pulsing for 4 hr and then stimulating them with high cAMP (300 μM) for another 14 hrs (Kim et al., 2002). Synchronous stimulation is a way of mimicking the *Dictyostelium* development (Sussman, 1987). In parallel with severe delay in development and drastic reduction in the size of the fruiting bodies, *DdLKB1* knockdown cells did not exhibit *CotB* and *D19* (*PspA*) prespore specific markers (Fig. 2.8A) at the time points tested. Spore enumeration from terminally developed structures revealed up to 80% reduction in number of spores in *DdLKB1* knockdown cells compared to wild type cells. Furthermore, there is drastic reduction in the prespore specific transcript levels during development as observed by the reduction of X-gal

staining region in slugs and fruiting bodies of *DdLKB1* knockdown cells in comparison with wild type cells, when *β-Galactosidase* was driven with prespore specific promoters. Together these results establish that DdLKB1 is necessary for normal formation of prespore cells during *Dictyostelium* development.

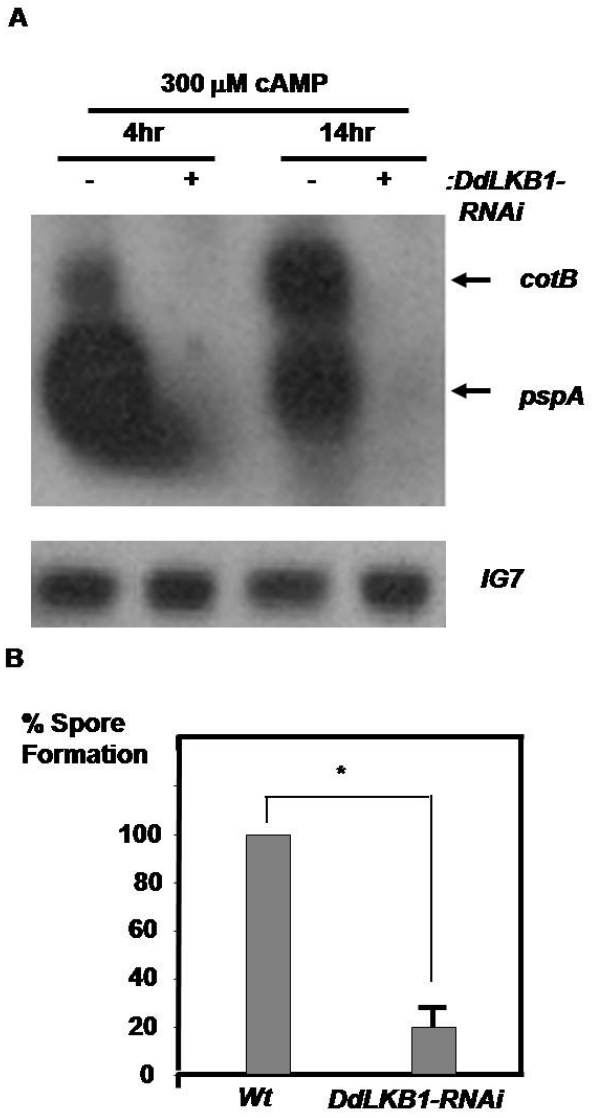

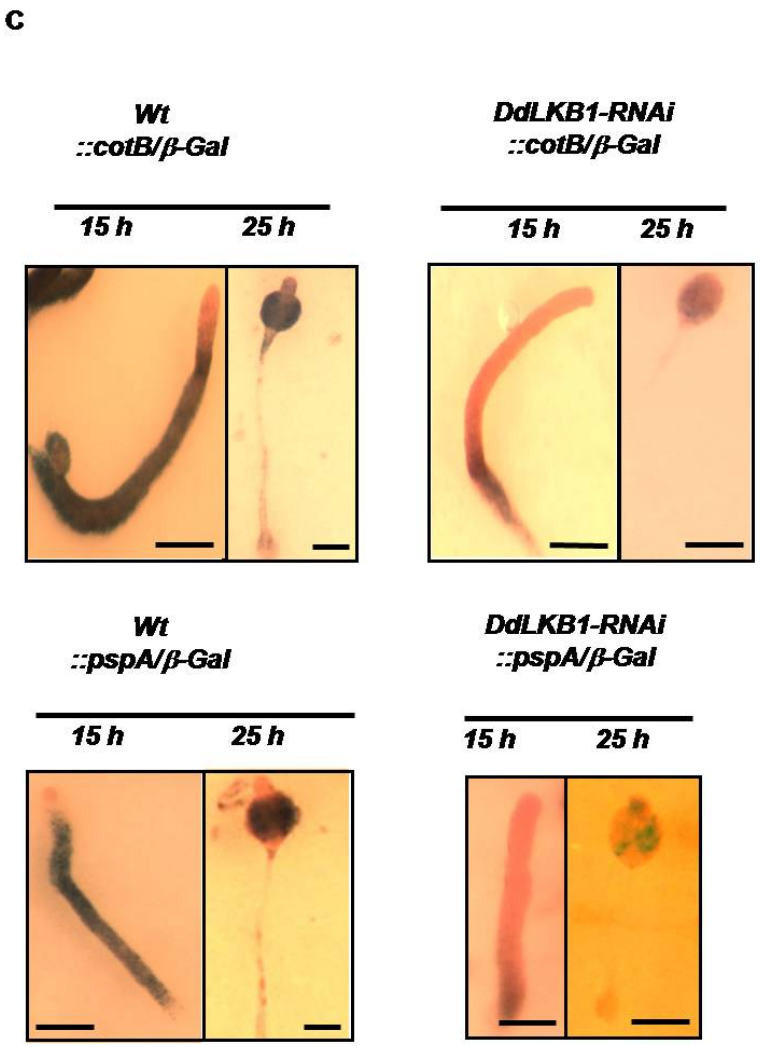

Figure 2.8 Effect of *DdLKB1* knockdown on prespore development. **A.** Northen blot assayed for prespore specific markers *CotB* and *PspA* in *DdLKB1* knockdown cells in comparison with wild tpye cells and IG7 was used as loading control. **B.** Spore count was done from terminally developed fruiting bodies of *DdLKB1* knockdown cells in comparison with wild type cells. The data is from three independent developments on nitrocellulose membranes. *p<0.0001, Student's t-test. **C.** Assay for prespore gene expression in *DdLKB1* knockdown cells in comparison with wild type cells.

β-Galactosidase was expressed from either *CotB* and *PspA* specific promoters either alone or along with *DdLKB1* knockdown construct in wild type cells and the extent of X-gal staining was compared in slugs and in fruiting bodies during development. All scale bars are 100 μm except the wild type fruiting body scale bar which are 62.5 μm.

2.2.7 Depletion of DdLKB1 results in decreased prespore to prestalk ratio

To further understand developmental defects exhibited by the *DdLKB1* knockdown cells, prestalk specific transcripts (*ecmA* and *ecmB*) were assayed by RT-PCR in both wild type cells and in *DdLKB1* knockdown cells. After normalizing for the IG7 transcript levels, *DdLKB1* knockdown cells displayed much higher levels of both *ecmA* and *ecmB* transcript levels especially at 4 hours of cAMP treatment (Fig. 2.9A). Decreased spore formation and excessive prestalk transcript levels suggested changes in prespore to prestalk ratio (80:20 in wild type cells) after depletion of DdLKB1 during development. To further confirm such changes, we expressed *β-Galactosidase* under the control of either of the two prestalk marker promoters (*ecmA* and *ecmB*) either alone or along with *DdLKB1* knockdown construct in wild type cells. These cells were developed on nitrocellulose membranes and assayed for X-gal staining. As shown in Fig. 2.9B, co-expression of *β-Galactosidase* along with *DdLKB1* knockdown construct resulted in increased prestalk staining which is extended to the prespore specific regions especially during fruiting body stage. On the contrary, expression of reporter constructs without DdLKB1 knock down construct resulted in normal prespore to prestalk ratio. These results strongly suggest that LKB1 is necessary for a proper prespore to prestalk ratio.

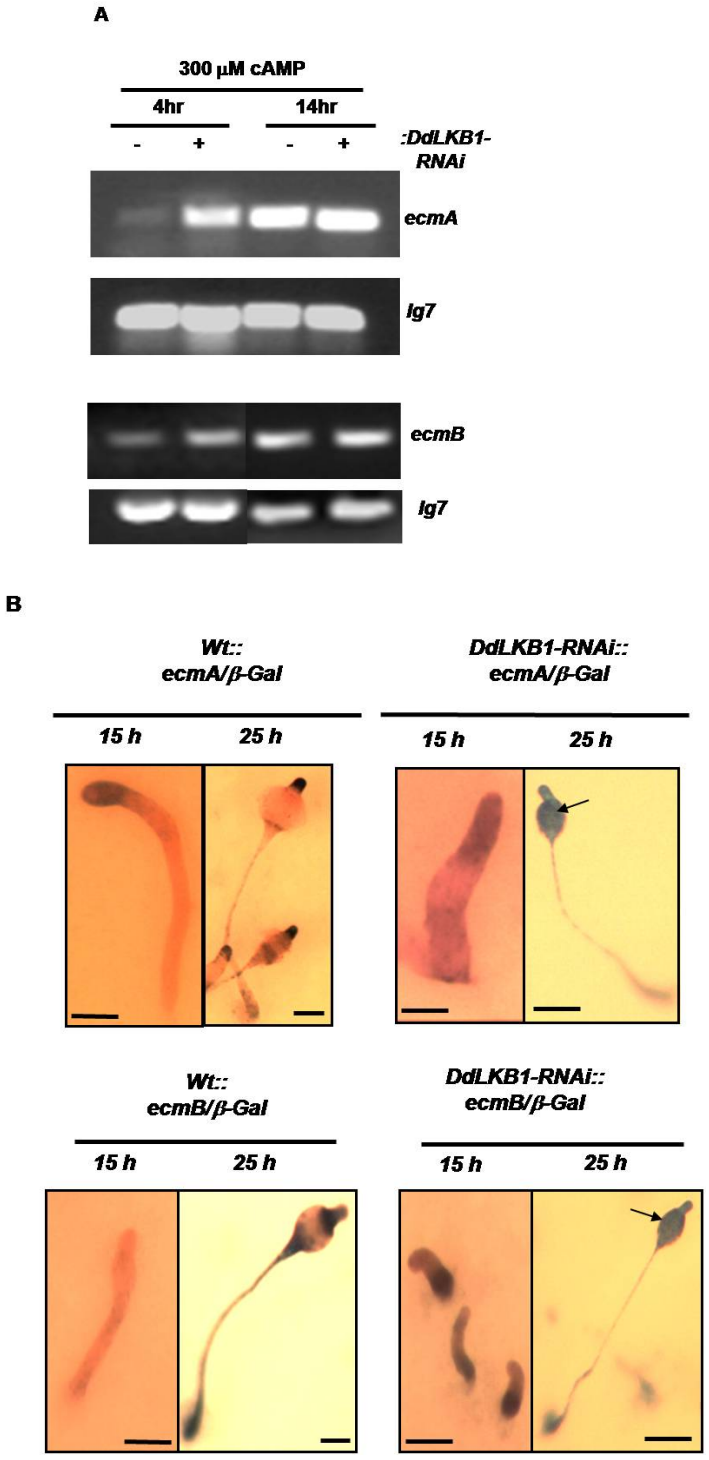

Figure 2.9 Effect of *DdLKB1* knockdown on prestalk development. **A.** Gels displaying amount of prestalk marker transcript levels in *DdLKB1* knockdown cells in comparison

with wild type cells as assayed by RT-PCR. Equal IG7 amplification shows the equal input of total RNA for the assay. **B.** Assay for prestalk gene expression in *DdLKB1* knockdown cells in comparison with wild type cells. *β-Galactosidase* was expressed either *CotB* and *PspA* specific promoters either alone or along with *DdLKB1* knockdown construct in wild type cells and the extent of X-gal staining was compared in slugs and in fruiting bodies during development. All scale bars are 100 μm except the wild type fruiting body scale bar which are 62.5 μm.

2.2.8 DdLKB1 is necessary for cAMP mediated GSK3 activation during evelopment

Developmental defects observed with *DdLKB1* knockdown were similar to the abnormalities observed in the absence of GSK3, suggesting a possible interaction between these two kinases. In order to test this hypothesis, GSK3 kinase activity was assayed from developmentally competent cells which were stimulated further with cAMP in both wild type and *DdLKB1* knockdown cells. Coincident with the phenotypic similarities, *DdLKB1* knockdown cells exhibited compromised GSK3 activity especially after four hours of high cAMP treatment where GSK3 activity was induced to the highest levels in normal cases along with low levels of tyrosine phosphorylation at Y214 when assayed with phospho-GSK3 antiserum after normalization for total GSK3 levels (Fig. 2.10 A and Fig 2.10B). As expected, *DdLKB1* knockdown lead to complete abolishment of the phospho-AMPK, a known LKB1 effector in higher metazoans, levels during development in contrast to wild type cells.

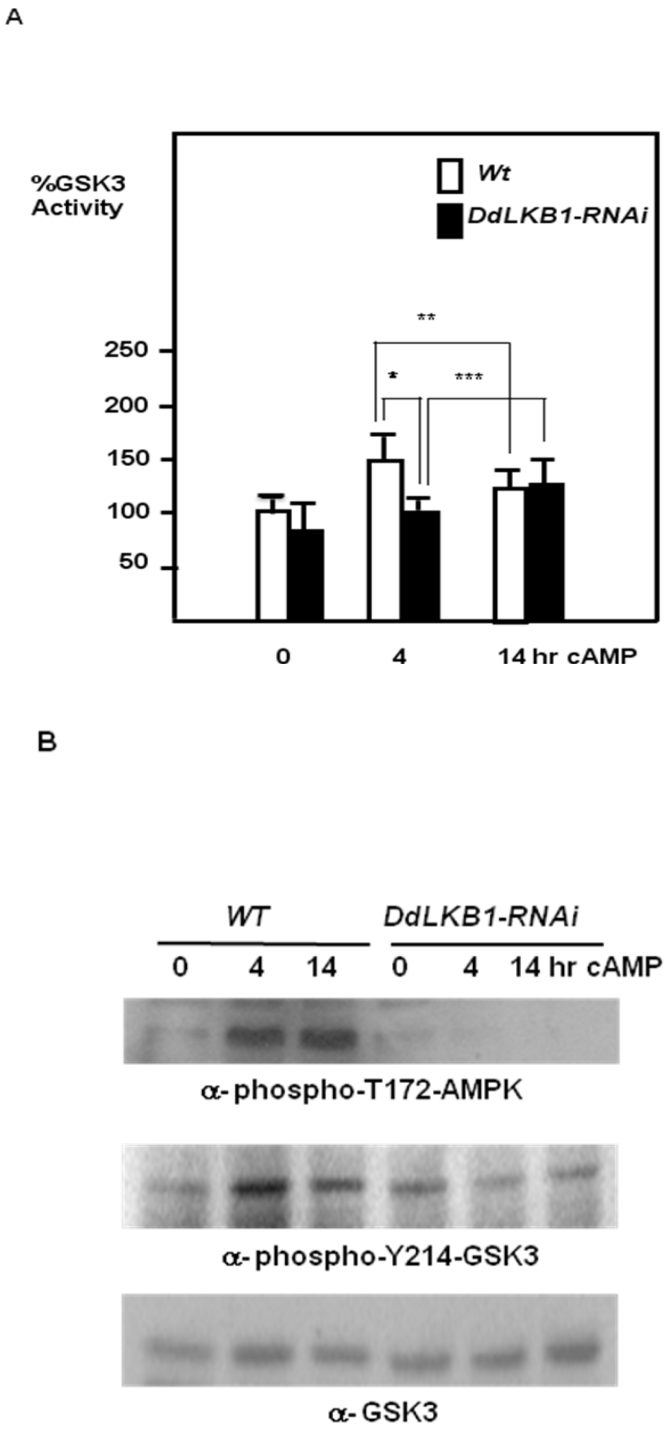

Figure 2.10 Molecular mechanisms of DdLKB1 function in *Dictyostelium* development. **A.** The extent of GSK3 specific kinase activity was displayed along with the error bars from *DdLKB1* knockdown cells when compared to wild type cells. The measurements are

the averages from three independent experiments. Nonspecific kinase activities from the LiCl treated samples were subtracted from original activites to calculate GSK3 specific kinase activity (Kim et al., 1999). All p values were calculated by Student's t-test. *$p<0.0001$, between wild type and *DdLKB1* knockdown cells at 4 hours of cAMP treatment, **$p<0.05$ between 4hr and 15hr wild type samples and ***$p>0.05$ between 4hr and 15hr *DdLKB1* knockdown samples. **B.** Western blot showing phospho AMPK and phospho GSK3 levels at various developmental time points in *DdLKB1* knockdown cells and in wild type cells. Total GSK3 levels were used to ensure equal cell lysate loading.

Previous studies have identified discrepancies in gene expression during the early stage of development in the absence of GSK3 when compared to wild type cells (Strmecki et al., 2007). The genes, which are important for *Dictyostelium* development, whose expression levels were altered in the GSK3 absence are: *ampA* (over expressed), and *dscA1* & *dscD1* (under expressed). To further confirm reduced GSK3 activity in *DdLKB1* knockdown cells, levels of these transcripts were assayed by RT-PCR. As shown in Fig. 2.11, *DdLKB1* knockdown cells showed similar expression pattern of these genes comparable to cells lacking GSK3. However, the levels of *car1*, another gene important during development, transcripts were not altered in *DdLKB1* knockdown cells as in *gsk3*$^{-}$ cells when compared to wild type cells, thereby underscoring the specificity of *DdLKB1* knockdown effect.

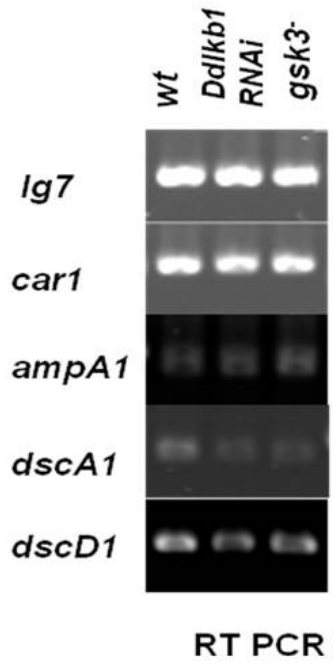

Figure 2.11 Similarities between *DdLKB1* knockdown and *gsk3*$^{-}$ in gene expression perturbation. Gel picture showing the transcript levels in *DdLKB1* knockdown cells, gsk3- cells in comparison with wild type cells. IG7 amplification served as control for equal RNA amounts across the lanes. All the genes assayed are induced during development and play a role in development.

2.2.9 DdLKB1 activity can be up regulated by various stress stimuli

As shown in Fig.2.12A, exposing cells to oxidative stress and osmotic shock resulted in around a two-fold increase in the LKB1 kinase activity. Consistent with an increased LKB1 activity, AMPK activity was also induced by stress signals as assayed by detecting phospho AMPK levels only in wild type cells but not in *DdLKB1* knockdown cells (Fig. 2.12B). These results suggest that LKB1 may regulate stress induced

responses through its down stream effector AMPK. However, there is no change in the phospho GSK3 levels in response to stress responses in wild type cells as well as *DdLKB1* knockdown cells.

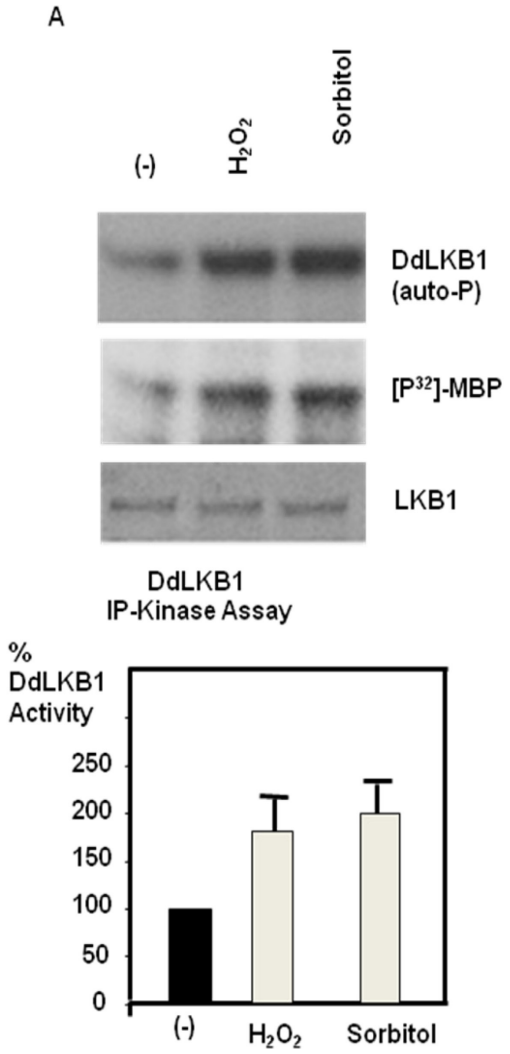

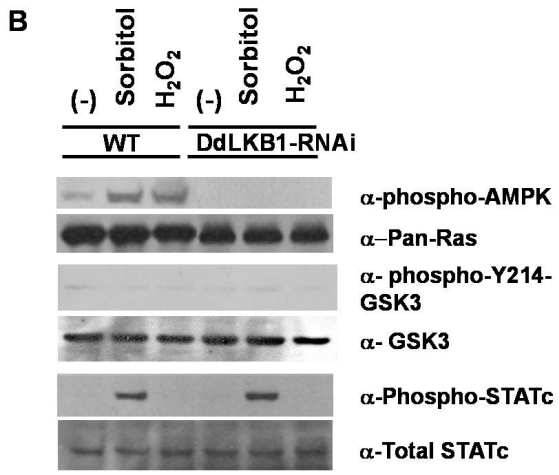

Figure 2.12 DdLKB1 response to stress stimulation and mechanisms of function. **A**. DdLKB1 kinase assay was done after exposing cells to oxidative stress and osmotic shock. Autoradiograms of LKB1 autophosphorylation and MBP phosphorylation and input MBP normalization after Coomassie staining were shown. The amount of DdLKB1 kinase activity was calculated based on the MBP phosphorylation status from three independent experiments and were depicted with error bars. **B**. Western blots showing phospho-AMPK levels, phospho-GSk3 levels, and phospho-STATc levels. All the western blots were performed on the same membrane after normalizing for pan Ras. Total AMPK input levels were assayed indirectly by probing for pan Ras levels.

2.3 Discussion and future directions

2.3.1 DdLKB1 is necessary for proper development of the *Dictyostelium*

Generation of knockout cell lines for a gene provides a unique opportunity to understand the function of the targeted gene. However, genes that are essential for cell growth and survival are proved to be difficult to be inactivated. Results from *DdLKB1*

konck-out trails suggested that generation of *DdLkb1* knockout cells was not realistic. It is likely that DdLKB1 is necessary for the survival of the organism, as it is the case in other metazoans (Ylikorkala et al., 2001). Conditional knockout approach using floxed *DdLkb1* constructs would be an alternative way by which future studies can solve this problem. In the current study, significant level of Dd-LKB1 down-regulation was achieved by RNAi-mediated knockdown approach. Furthermore, an epitope-tagged DdLKB1 was generated that allowed an in vitro kinase assay to measure DdLKB1 activity under various situations.

As previously described, DdlKB1 is enriched in the prespore cells and its activity is up-regulated during development. Moreover, after depletion of DdLKB1 by RNAi, it was revealed that DdLKB1 is crucial for proper spore formation and results in altered prespore to prestalk cell ratios along with delay of development. The above results, together with the DdLKB1 expression pattern (confined to prespore lineage), may indicate that DdLKB1 is important for prespore cell development. It is important to further confirm the expression of DdLKB1 during development. *In situ* hybridization or RT-PCR for *DdLkb1* from the fractioned prestalk cells will further confirm these results.

To understand the mechanism by which DdLKB1 kinase activity is up regulated during development, the ability of the two morphogens cAMP and DIF-1 to induce DdLKB1 kinase activity was tested. Though both of these morphogens positively influenced DdLKB1 kinase activity, but it is still not known how DdLKB1 kinase activity is induced during development, as the up regulation in kinase activity by the two morphogens is almost half of that observed during normal development. Also, there is no immediate up regulation after stimulation. Moreover, the mechanism of action of these

two morphogens is not similar. cAMP relays its effects through cARs, and the mechanism by which membrane permeable DIF-1 influences development is largely unknown. The other noteworthy morphogen that can be tested to induce the DdlKB1 activity up-regulation during development is prespore-inducing factor [psi (ψ) factor] (Kawata et al., 2004). It is also possible that additional mechanisms might exist in up-regulation of DdLKB1 kinase activity during development, or up-regulated DdLKB1 activity could be due to a lack of suppression during development. Based on its sequence analysis, DdLKB1 consists of one PKA consensus phosphorylation site at its C-terminus and one PKB consensus phosphorylation site at its N-terminus (Fig 2.1A). It is possible that LKB1 might be regulated during development by the PKA and/or PKB. Generation of point mutants at these consensus phosphorylation sites will help to substantiate this possibility.

As suggested by the close resemblance of the developmental phenotypes induced by DdLKB1 knockdown to those exhibited by *gsk3*$^{-}$ cells, a functional interaction between LKB1 and GSK3 at the molecular level was observed. The above results indicate that DdLKB1 is necessary for activation of GSK3 kinase activity during development. This result is in contrast to the role of LKB1 during *Xenopus* development where LKB1 potentiates Wnt signaling by inhibiting GSK3 indirectly (Ossipova et al., 2003). However, it remains to be determined how DdLKB1 is able to increase/maintain GSK3 Y214 phosphorylation and cause the up-regulated GSK3 activity during development. Probably, DdLKB1 might activate ZAK1, which was shown to phosphorylate GSK3 at Y214 to activate its kinase activity. Alternatively, DdLKB1 might suppress a tyrosine phosphatase, thereby maintaining the GKS3 kinase activity

during development. Evaluation of these two hypotheses will aid in identification of GSK3 regulation, which is central to many important cellular functions.

Depletion of DdLKB1 during development also interfered AMPK phosphorylation. A previous study (Bokko et al., 2007) has shown that inhibition of AMPKα by antisense mechanism resulted in defective aggregation as well as much smaller and fewer fruiting bodies. Our results further corroborate those findings by suggesting that failure of AMPK activation in *DdLKB1* knockdown cells led to the inefficient aggregation and the formation of fewer and smaller fruiting bodies. It would be interesting to know the spatial expression pattern of AMPKα to further understand its developmental role in tandem with DdLKB1.

2.3.2 DdLKB1 might regulate energy balance during stress

Apart from its developmental role, DdLKB1 also plays a role in mediating stress responses. Phospho-AMPK levels were induced by stress stimulation in wild type cells but not in *DdLKB1* knockdown cells, implying that DdLKB1 is essential for stress induced activation of AMPK. It is possible that LKB1 is activating the AMPK in response to stress, thereby suppressing protein synthesis in order to conserve energy and to cope with the stress. Inhibition of the TOR (Target of rapamycin) pathway through AMPK could be one such pathway suppressing protein synthesis. However, GSK3 is not activated in response to stress in wild type cells, suggesting the possibility of a differential DdLKB1 function in regulation of GSK3 during development and during stress. It is also possible that other GSK3 activators are not activated by stress stimulation. *DdLKB1* knockdown cells did not deviate from wild type cells in phospho-

STATc levels in response to osmotic shock, suggesting that DdLKB1 is not involved in the STATc mediated regulation of gene induction during osmotic shock. It is possible that LKB1 might be operational through translational regulation by AMPK/TOR pathways rather than transcriptional regulation in mediating osmotic responses.

To better understand the mechanisms by which DdLKB1 is regulating its developmental and stress response functions, it is necessary to characterize the LKB1 partners such as STRAD and MO25 in *Dictyostelium*. Though *Dictyostelium* has the putative homologues of STRAD and MO25, no information is available with regard to their function. The genes DDB0229911 and DDB0230012 share 46% and 45% homology with STARDα and STRADβ, and DDB0218587 shares 74% homology with MO25. Generation of single and multiple knockouts of these genes and delineation of affect of absence of those proteins on DdLKB1 kinase activity will further elaborate the up regulated LKB1 kinase activity during development and during stress insults. Such studies may also aid in understanding the differential regulation of GSK3 activity by the DdLKB1 during development and stress.

2.3.3 Significance

The present study was aimed towards understanding the function of LKB1, with proven roles in cancer and in regulation of development, in a model organism *Dictyostelium*. My study capitalizes on the model organism's tractability and simplicity, and attempts to establish the location of this significant protein, in a known cascade of events that regulate the responsiveness of cells to various stimuli and developmental programming that generates developmental multicellularity. Establishment of such

hierarchies and understanding of the nature of LKB1 regulation will not only add a piece to the puzzle but also enable us to design efficient ways of targeting and modulating cell growth and proliferation in pathological cases such as cancers.

Chapter 3

THE GPI-ANCHORED SUPEROXIDE DISMUTASE SODC IS ESSENTIAL FOR REGULATING BASAL RAS ACTIVITY AND FOR CHEMOTAXIS OF *DICTYOSTELIUM DISCOIDEUM*

3.1 Materials and methods

3.1.1 Generation of Restriction Enzyme Mediated Insertion (REMI) mutants and *sodC*$^-$ cells

Remi clones were generated following the Terminator Trapping REMI protocol (Takeda et al., 2003) from Ax3 cells expressing the GFP-PHcrac protein. Individual *Remi* clones were identified using the 3' Race Core Kit (TAKARA): the cDNAs were generated from RNA by RT-PCR with the oligo dT-3 sites adaptor primer from the 3' Race kit, and then amplified by PCR using a Blasticidin specific primer (5'-CGAGTGGTAAGTCCTTGT GG-3') and the oligo dT-3 adaptor primer. The Blasticidin cassette was identified at the 1004th nucleotide of the *SodC* open reading frame in *remi56*. Three other independent *Remi* clones also contained the Blasticidin cassette at the identical position of *SodC*. *sodC*$^-$ cells were generated by homologous recombination from wild type cell (*JH10*), and confirmed by genomic PCR using a primer set (5'-GGTGGTGTTGAAGGTATT-3' and 5'-TTCAACATTACCACCATTTGC-3'). The absence of *SodC* transcript was confirmed by RT-PCR using the following primer set 5'-ATGAGACTTTTATCTGTA TTAG-3' and 5'-TTAAAGCAAAGCAAAGATAATTG-3'.

3.1.2 Generation of the full length *SodC*, *GFP-SodC*, and *myc-SodC* constructs

The full length *SodC* was cloned by RT-PCR using the primer set 5'-ATGAGACTTTTATCTGTATTAG-3' and 5'-TTAAAGCAAAGCAAAGATAATTG-3', and confirmed by sequencing. GFP-SOD was constructed by excising the SOD domain from full length SodC in the TOPO-TA vector by HinCII digestion and

subcloned into the PGEX-4T-2 vector (Pharmacia). The SOD domain was then excised using EcoRI and AccI, and subcloned in-frame into the *Dictyostelium* GFP expression vector, pDEXH-GFP (Faix et al., 1992). The construct was confirmed by sequencing and expression was verified by western blotting with anti-GFP antibody (1:1,000, Covance, Inc).

Myc-SodC expression plasmid was constructed as follows. The full length *SodC* cDNA in TOPO vector was amplified with M13 primer and a primer encoding SodC Signal Peptide (SP) / Myc sequence and NdeI site (CCATATGTTAAATCTTCTTCTGA AATTAATTTTTGTTCAAAAGCATATTGGTAATCGGCTTTTGCAATGGAAATAC 3'), subcloned into a TOPO vector (pTOTP-SP-Myc-Nde1), and confirmed by sequencing. Both pTOPO-SodC and pTOPO-SP-Myc-Nde1 were digested with Xho1 (TOPO vector) and Nde1 (at 211th bp of SodC) and gel purified. The SP-Myc-Nde1 (153bp) insert was ligated to the digested vector to create Topo-SP-Myc-SodC, in which a Myc epitope replaced 124 bp (76~210 nt) of SodC. After sequence confirmation, the SP-Myc-SodC was released with EcoR1 digestion and ligated to EcoR1 digested pExp4 vector to create SP-Myc-SodC.

A *SodC* mutant with a disrupted copper-binding site (*SodC(H245R, H247Q)*) (Wang et al., 2002) were generated with a mutant primer (ccggtttatcttatcaagctcatggtttc AGAgttcAACaatttggtgatgtttcatcgg, where capital letters denotes mutations) and the Quickchange site directed mutagenesis kit (Stratagene).

3.1.3 SOD activity assay

Assay for SOD activity was done using the SOD assay kit (Dojindo, Inc.) according to the manufacturer's instructions. The WST-1 solution (200 μl) was mixed with the Xanthine Oxidase-containing enzyme mix, (20 μl) and the SOD containing samples (20 μl) and were incubated at 25°C for 15 minutes. The relative superoxide levels were determined by measuring the OD_{450} of the reaction mix after 20 minutes at 25°C. The WST-1 formazan has a molar absorptivity of 3.7×10^4 at 450 nm. Mean values from three independent experiments are shown with error bars representing standard deviations.

For testing GPI cleavage of SodC, cells were treated with phosphatidylinositol specific phospholipase C (PI-PLC, Molecular Probes) prior to the SOD assay. For these, 1×10^6 log phase cells were washed and resuspended with 200 μl of 1X PBS. 10 μl of PI-PLC (1.0 Unit) was added to each sample, and the reaction mixtures were incubated at 25°C for 5 minutes. The cell free media were saved and their SOD activities were measured as described above. Mean values from three independent experiments are shown with error bars representing standard deviations.

3.1.4 Superoxide quantification: XTT and NBT assays

Extracellular superoxide levels were measured by using XTT as described previously (Bloomfield and Pears, 2003). The cells (10^8) were pulsed with 50 nM cAMP for 4 hours at 20×10^6 cells/ml. Equivalent amount of cells (~1.5×10^7) were harvested and resuspended with 0.15 ml of DB containing 0.5 mM XTT for 10 minutes at 22°C. The amount of reduced XTT was measured spectrophotometrically at 470 nm.

Levels of intracellular superoxide were measured by using NBT (Nitro blue tetrazolium salt) as previously described (Choi et al., 2006). The cells at the density of 2 x 10^7 cells/ml were pulsed with 50 nM cAMP for 4 hours, and resuspended with 1ml of DB containing 0.2 mM NBT for 30 minutes at 22^{o}C. Cells were then washed twice with DB, once with methanol, and air-dried. Dried pellets were solubilized with 0.24 ml of 2 M KOH and 0.28 ml of DMSO (dimethyl sulfoxide). The intracellular NBT extracted from cells were measured spectrophotometrically at 620 nm.

3.1.5 Submerged aggregation and cAMP chemotaxis assays

For submerged aggregation experiments, log phase cells were harvested, washed and placed under DB at the cell densities of 2.5x10^4 cells/cm^2. After 10 hours at 22^{o}C, cell migration, streaming, and aggregation were observed.

For chemotaxis assays, log phase cells were differentiated with 50 nM pulses of cAMP for 4 hrs. Aggregation-competent cells were plated at a density of 6x10^4 cells/cm^2. A micromanipulator with a glass capillary needle (Eppendorf Femtotip) was filled with either 100 nM or 10 μM cAMP solution. The responses of the cells were followed by time-lapse video recording using a CoolSNAP digital camera. The roundness of a chemotaxing cell, which represents polarity of cells, is defined as the ratio of ellipsoidal short radius divided by its long radius was calculated as described elsewhere (Loovers et al., 2006). Chemotactic index, defined as the distance moved in the direction of the pipette divided by the total distance moved, was computed from the centroid positions (Loovers et al., 2006).

3.1.6 Fractionation of the membrane and cytoplasm

Fractionations of cells expressing GFP-PH_{CRAC} proteins were described else where (Parent et al., 1998). 10^7 vegetative cells were washed and resuspended with 150 µl of membrane lysis buffer (20 mM TrisCl, pH 7.7, 2 mM $MgSO_4$) and filter-lysed into 1 ml of cold PM buffer (5 mM KH_2PO_4, 5 mM Na_2HPO_4, 2 mM $MgSO_4$) by filtration through a Nucleopore filter (0.2 µm). Cell lysates were immediately centrifuged at 12,000 x *g* for 1 minute at 4°C to separate the membrane containing pellets from the cytosolic supernatant fractions. The supernatant was mixed with 4X SDS loading dye and the pellets were solubilized with 50 µl of 1X SDS loading dye. 10 µl of the membranous fractions and 20 µl of the cytosolic fractions were separated on a 4-20 % gradient SDS-PAGE. GFP-PH_{CRAC} localization was analyzed by western blotting using an anti-GFP antibody (1:1,000, Covance Inc).

The PI3K containing membranous fractions were prepared according to the published procedures (Han et al., 2006; Sasaki et al., 2004). 2.5 x 10^7 cells were resuspended with 200 µl of 1x PBS and mixed with an equal volume of 0.02% of Triton X-100 solution and incubated on ice 5 minutes. All solutions contained protease inhibitors (Roche, Complete Mini). Mixtures were, then, centrifuged at 12,000 x *g* for 5 minutes at 4°C. The cytosolic supernatant fractions were separated from the membranous pellet fractions. The supernatants were mixed with 4X SDS loading dye and the pellets were solubilized with 100 µl of 1X SDS loading dye. 1 µl of the membranous fractions and 40 µl of the cytosolic fractions were analyzed by western blot using anti-GFP antibodies described above.

3.1.7 GFP-fusion proteins and immunofluorescence microscopy

The N-PI3K1-GFP and GFP-RBD constructs were described earlier (Sasaki et al., 2004). All fluorescent images were obtained using a 100X oil lens on a Leica DM IRB inverted epifluorescence microscope. For indirect fluorescence microscopy, cells were permeabilized with 0.01% Triton X-100 in 1 x PBS for 10 minutes, and fixed with 3.7% formaldehyde for an additional 20 min at 22^{o}C. Fixed cells were washed twice with 1 X PBS, then incubated with an anti-Myc antibody (1:100 dilution, Santa Cruz Biotech) for an additional 2 hours at 22^{o}C, and washed three times with 1 x PBST (1 x PBS, 0.3% Triton X-100) for 30 min at 22^{o}C. Rhodamine-conjugated anti-Rabbit goat IgG (1:200 dilution, Molecular probes) was used as a secondary antibody.

3.1.8 Antibodies

Anti-GFP antibodies were from Covance for western blot analysis (1:1,000 dilution) and from eBioscience for immunoprecipitation (5 µl per each IP). Anti-Myc and anti-Pan-Ras antibodies were from Calbiochem (Ab-3).

3.1.9 Ras binding assay

Ras assays were as described by Sasaki et al. (2004). Cells were pulsed with cAMP for 4 hours and then lysed with cell lysis buffer (20 mM TrisCl [pH7.7], 150 mM NaCl, 1% Triton X-100, 5% glycerol, 1 mM EDTA, 0.1 %beta-mercaptoethanol, and 1x Roche Protease Inhibitor mix). The whole cell lysates were then mixed with 5 µg of purified GST-RBD (Ras Binding Domain) on Glutathione-sepharose beads for 2 hours at 4^{o}C with, and the GST-RBD/active Ras complexes were washed three times with cell

lysis buffer. The active Ras proteins bound with GST-RBD were visualized by western blotting with anti-Pan-Ras antibody (Calbiochem, Ab-3). Wild type and *sodC*$^-$ cells expressing GFP-RBD proteins were pulsed with 50 nM cAMP in DB for 4 hours and monitored under epifluorescent microscope.

3.1.10 Ras activation with conditioned medium (CM)

A previous study showed cellular superoxide production in response to stimulation with conditioned medium prepared after cAMP pulsing (Bloomfield and Pears, 2003). One hundred million cells in 5 ml DB were pulsed with 50 nM cAMP pulses for 4 hours, and the supernatant fraction was saved as the conditioned medium (CM) after separation of cells by centrifugation. Ras activation in response to superoxide generation was determined by GST-RBD assay as described earlier. Superoxide radicals were depleted by incubation with the scavenger XTT (4 mM). Ras activation was measured by GST-RBD assay as described above.

3.1.11 F-Actin assay

Cells were cAMP pulsed at 2 x 10^7 cells/ml for 4 hours, briefly centrifuged, and resuspended with PM buffer (5 mM KH_2PO_4/K_2HPO_4, 2 mM $MgCl_2$) at 3 x 10^7 cells/ml. Cells were stimulated with 10 μM cAMP four times as indicated at the figure legends. At each time point, 100 μl of cells were taken and mixed with 1 ml of Actin buffer (3.7% formaldehyde, 10 mM Pipes, 0.1% Triton X-100, 20 mM K_2HPO_4/KH_2PO_4, 5 mM EGTA, 2 mM $MgCl_2$, 250 nM TRITC-phalloidin, pH 6.8). Cells were fixed and stained for 1 hour at 21^{o}C on orbital shaker. Cytoskeletal fractions were pelleted by

centrifugation and washed with 1ml of Methanol and shaken overnight. Methanol extracted TRITC-phallodin was quantified by fluorimetry (540-nm excitation, 575-nm emission).

3.1.12 F-Actin staining with TRITC-Phalloidin

Both wild type and *sodC*$^-$ cells were pulsed at 2 x 10^7 cells/ml in DB for 4hr. Cells were plated on 8 well chambers at a density of 100 x 10^3 per cm^2 and incubated for 5 min at 22^{o}C. Then cells were washed twice gently with 1xPBS. Fixation was done by adding 3.7% formaldehyde in 1 x PBS for 10 min at 22^{o}C. Subsequently, cells were permeablized with 0.01% Triton X in PBS for 5 min at 22^{o}C. The cells were washed three times with 1 x PBS before the addition of 1xPBS containing 0.5 μM TRITC-Phalloidin and 0.5 % BSA. After 30 minutes of incubation at 22^{o}C, cells were washed three times with PBS and examined under fluorescent microscope.

3.2 Results

3.2.1 Generation of REMI mutants exhibiting higher constitutive levels of PIP3

To find additional components involved in the regulation of PIP3 level, wild type cells expressing GFP-PHcrac were randomly mutagenized by the Terminator Trapping REMI method (Takeda et al., 2003). The marker, GFP-PHcrac has previously been shown to bind PIP3 and has been used as a marker for PIP3 localization (Huang et al., 2003). Out of ~1,000 independently isolated insertional mutants, six independent *remi* clones exhibited elevated level of GFP-PHcrac at the plasma membrane in the absence of chemoattractant stimulation (Fig. 3.1A). In contrast, GFP-PHcrac proteins were localized

uniformly through the cytoplasm and occasionally enriched at the local membrane ruffles and macropinosomes in wild type cells. It is expected that the mutants displaying higher PIP3 levels would be severely defective in chemotaxis. One such example is *pten*$^-$ cells, which show severe defect in chemotaxis (Funamoto et al., 2002, Iijima and Devreotes, 2002). *remi56* cells, as a representative of *REMI* mutants, failed to form territorial streams when tested by under-buffer aggregation assay (Fig. 3.1B).

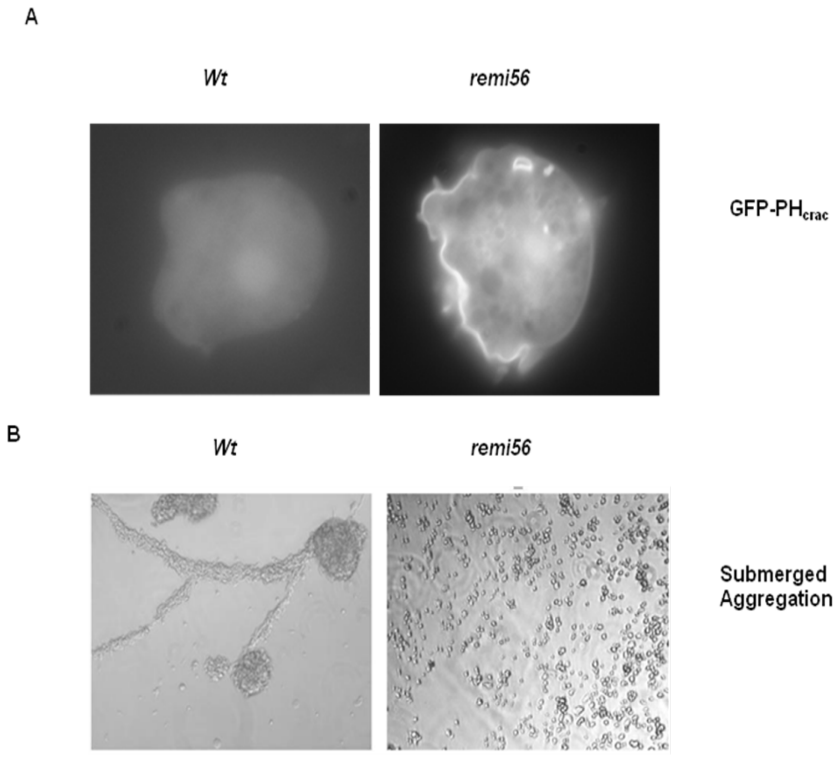

Figure 3.1 Generation of REMI mutants exhibiting higher basal levels of GFP-PHcrac at the plasma membrane. **A.** *remi56* cells displayed more plasma membrane localization GFP-PHcrac, which suggesting higher PIP3 levels in the membrane of *remi56*. **B.** Wild type and *remi56* lines were tested to see if they are able to form developmental territorial

streams. *remi56* lines failed to aggregate in submerged culture at the cell density of 2.5 x 10^4 cells/cm^2, where wild type cells aggregated normally.

3.2.2 Identification and characterization of *SodC*

Insertion loci were identified as described in the Materials and Methods. The mutant cell line, *Remi 56* as well as three other mutants had insertions at the same locus encoding an extracellular superoxide dismutase (SOD) previously identified as *SodC* (Tsuji et al., 2003). The message, *SodC* was expressed both in vegetative and aggregative stages, and gradually declined as cells terminally differentiate (Iranfar et al., 2003; Van Driessche et al., 2002). Sequence analysis of *SodC* revealed a signal peptide as previously suggested (Tsuji et al., 2003), and a previously undescribed carboxyl terminal glycosylphosphatidylinositol (GPI) anchoring motif (Fig. 3.2A). Interestingly, *SodC* encodes an incomplete SOD domain near the amino-terminal end in addition to a complete SOD near the C-terminus. Three independent *sodC*$^-$ cells were generated by homologous recombination and confirmed by genomic PCR analysis (Fig. 3.2B). *sodC*$^-$ cells were transfected with a GFP-PHcrac expression construct to indirectly assess the level of PIP3. *sodC*$^-$ cells exhibited significantly more GFP-PHcrac protein at the plasma membrane than wild type cells similarly to *remi56* (Fig. 3.2C). Aberrant plasma membrane localization of the GFP-PHcrac proteins in *sodC*$^-$ cells was further confirmed by subcellular fractionation. The membrane and cytosolic fractions were prepared from wild type and *sodC*$^-$ cells using membrane filters (Parent *et al*., 1998), and analyzed by western blotting using an anti-GFP antibody. Consistent with the GFP images, significantly more GFP-PHcrac protein was detected in the membrane fraction of the

sodC⁻ cells (Fig. 3.2D). As a control, the same blot was re-probed with a pan-Ras antibody. As expected, most Ras proteins were detected from membrane fractions. These data suggested that both *remi56* and *sodC*⁻ cells might have constitutively higher levels of PIP3.

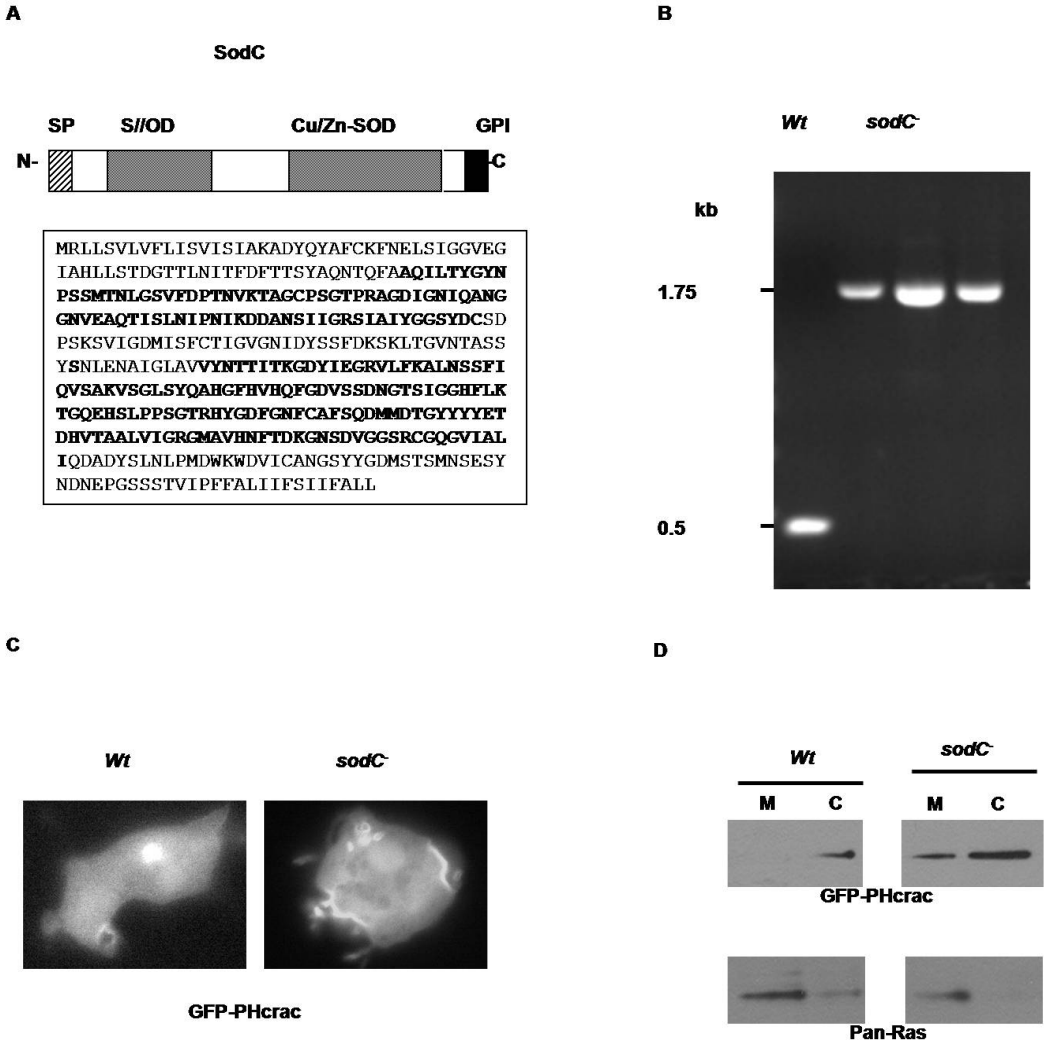

Figure 3.2 Identification of insertional mutation in the REMI mutants and generation of *sodC*⁻ cells. **A.** *remi56* displayed an insertion at a locus encoding a superoxide dismutase (SOD) domain containing protein, SodC. *SodC* encodes an N-terminal signal peptide with the C-terminal GPI anchoring sequence (Omega domain), a partial and a full Cu/Zn-

superoxide dismutase (SOD) domain. **B.** *sodC*$^-$ cells were generated by homologous recombination from wild type cells, and confirmed by genomic PCR. **C.** *sodC*$^-$ cells showed increased basal membrane localization of GFP-PHcrac than wild type cells. **D.** Western blot analysis of the cytosolic and membrane fractions of the wild type and *sodC*$^-$ cells showed more GFP-PHcrac localization at the membrane in *sodC*$^-$ than wild type cells. Ras proteins were shown as a loading control for membrane fractions.

3.2.3 *SodC* encodes superoxide dismutase with a GPI anchor

The Cu/Zn-SOD domain of SodC was expressed as a GFP fusion protein under the Actin-15 promoter and detected by anti-GFP antibody (Fig. 3.3A). When incubated with superoxide radicals, the GFP-SOD domain inhibited superoxide-dependent Formazan formation whereas the same amount of GFP control showed little inhibition (Fig. 3.3B).

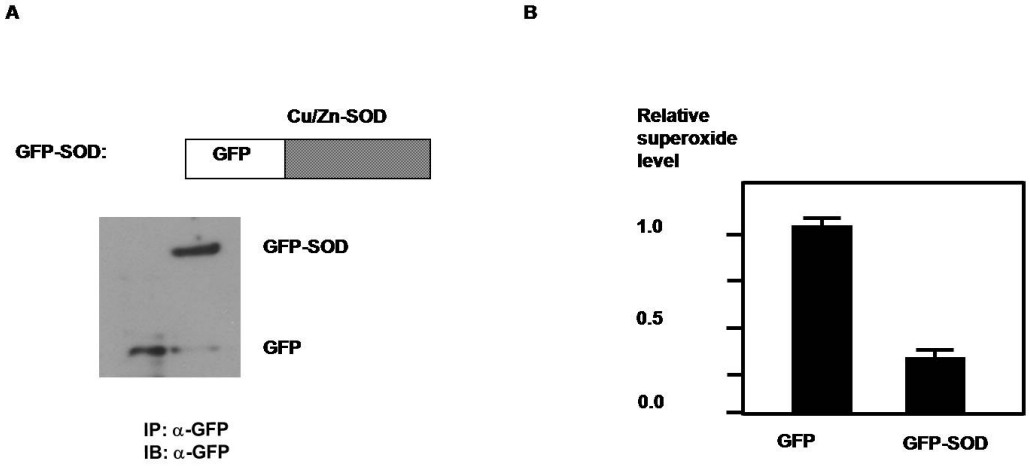

Figure 3.3 SodC has SOD activity. **A.** The SodC SOD domain was expressed in *Dictyostelium* as GFP fusion proteins under the Actin 15 promoter. GFP and GFP-SOD

proteins were purified by immunoprecipitation with anti-GFP antibody, and normalized by western blot analysis using anti-GFP antibody. **B.** Relative superoxide levels were compared after incubation with equal amount of purified GFP or GFP-SOD protein. The relative superoxide level from GFP was set as 1.0. GFP-SOD samples exhibited an average level of 0.3 (standard deviation of 0.06) from three independent experiments.

To consolidate that SodC is actually a GPI-anchored membrane protein, a *Myc*-tag was inserted after the signal peptide of the full length *SodC*. Myc-SodC proteins were immunopurified and detected by anti-Myc antibody (Fig. 3.4A, bottom left). Membrane localization of Myc-SodC was evident from both western blotting of subcellular fractions (Fig. 3.4A, bottom right) and indirect immunofluorescence microscopy (Fig. 3.4B). To further test if there is a GPI anchored SOD activity, wild type cells were treated with GPI specific phosphatidylinositol-phospholipase C (PI-PLC) (Kondoh *et al*., 2005). The media from PI-PLC treated wild type cells displayed three times higher SOD activity than that of the control (Fig. 3.4C). In contrast, the media from *sodC*$^-$ cells displayed no measurable amounts of SOD activity under the same experimental conditions.

Being localized on the outer leaflet of the plasma membrane through GPI anchor, SodC may control extracellular superoxide level and/or penetration of the radical across the plasma membrane, and thus intracellular superoxide level. When tested by the previously published assay method using superoxide sensitive reagent XTT (Bloomfield and Pears, 2003), wild type and *sodC*$^-$ cells displayed no significant difference in the level of extracellular superoxide level as shown in figure 3.4D.

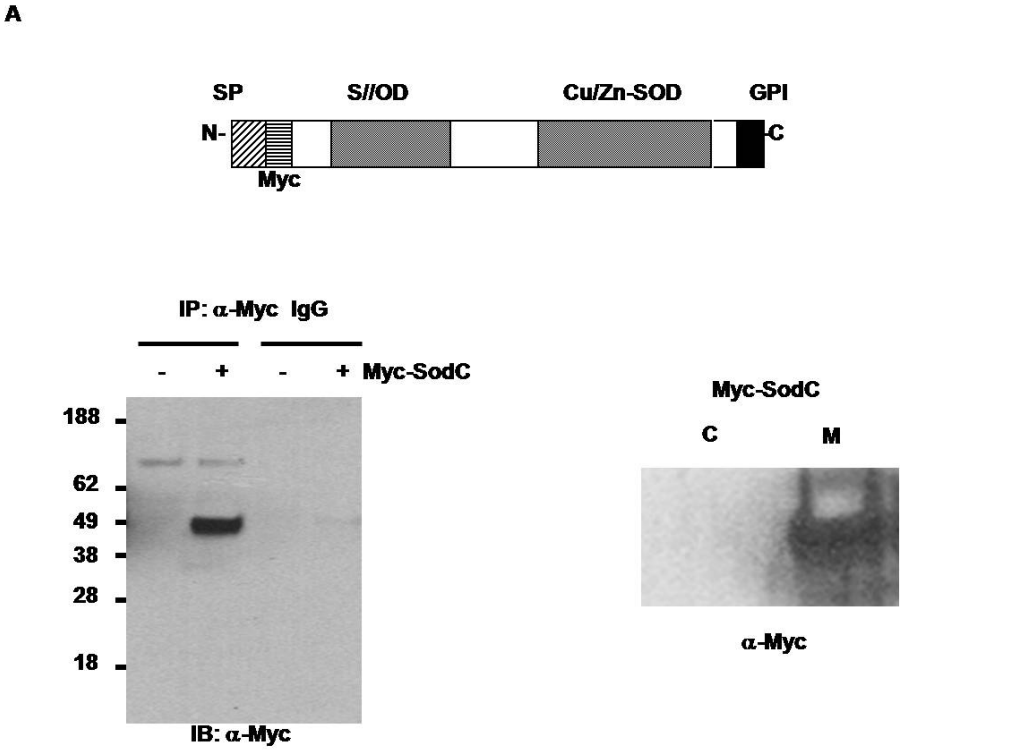
A
SP
S//OD
Cu/Zn-SOD
GPI
N-
C
Myc
IP: α-Myc IgG
- + - + Myc-SodC
188
62
49
38
28
18
IB: α-Myc
Myc-SodC
C
M
α-Myc
B
Myc-SodC/Wt
IgG
α-Myc
C
Relative SOD Activity
3.0
2.0
1.0
0
PI-PLC: - + - +
Wt
sodC-

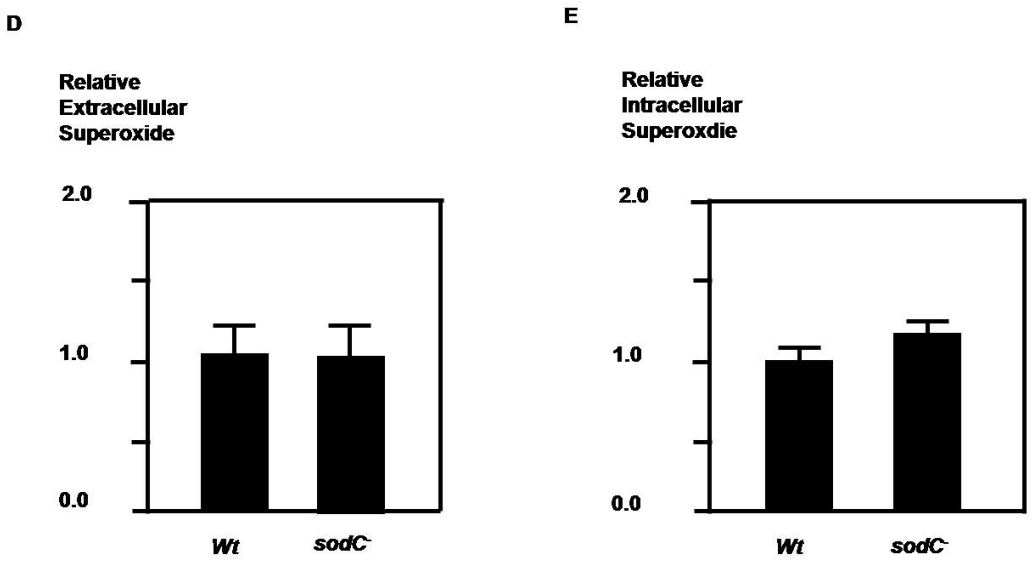

Figure 3.4 SodC is a GPI-anchored membrane protein. **A.** A Myc epitope tag was inserted in frame after the SodC signal peptide. Myc-SodC was expressed in the wild type background, and detected by western blotting (bottom left). Membrane and cytosolic fractions were prepared, and Myc-SodC was detected only from the membrane fraction. **B.** Membrane localization of Myc-SodC was also confirmed by indirect immunofluorescence. **C.** Log phase wild type and *sodC*$^-$ cells were plated at a density of 1 x 10^6 cells/cm^2, and treated with or without 1 unit of GPI specific PI-PLC for 5 minutes at 25^{o}C, and extracellular SOD activities were compared. **D.** The relative levels of extracellular superoxide of wild type and *sodC*$^-$ cells were measured using XTT reduction as described in the materials and methods section. Virtually identical levels of the radical were detected from three independent experiments. **E.** The relative intracellular superoxide levels were determined by using NBT. Cell-trapped NBT were ~18 % ($\pm$5% SD) higher in *sodC*$^-$ than wild type cells from three independent experiments.

Next, the intracellular superoxide levels were measured by using another superoxide sensitive reagent NBT. Contrary to XTT, NBT becomes an insoluble precipitate upon reduction by the radical (Choi et al., 2006). The amount of insoluble NBT trapped inside the *sodC*$^-$ cells was consistently higher by ~ 18 % than that in the wild type (Fig.3 4E). These data suggest that SodC is a GPI-anchored Superoxide Dismutase involved in the regulation of intracellular level of superoxide in *Dictyostelium* cells.

3.2.4 *sodC*$^-$ cells are defective in chemotaxis but not development

Like *remi56*, *sodC*$^-$ cells were severely defective in aggregation (Fig. 3.5A). However, when plated at high cell densities where chemotaxis is less essential, *sodC*$^-$ cells developed indistinguishably from wild type cells (Fig. 3.5B). These data strongly suggested that SodC is essential for chemotaxis but not so for development.

Cells lacking *SodC*, after being pulsed for 4 hours, displayed a significantly compromised chemoattractant sensing during the first 20 minutes under both weak and strong cAMP gradients (Fig. 3.6B and 3.6C). However, during the second 20 minutes under both weak and strong cAMP gradients, *sodC*$^-$ cells showed an improvement in cAMP sensing, but only up to ~ 40 % of the wild type level (Fig 3.6A). In addition, *sodC*$^-$ cells showed severe motility defects, which was worse under weak cAMP gradient (Table 3.1). Contrary to the chemotaxis index, the speed of motility did not improve during the whole duration of the assay.

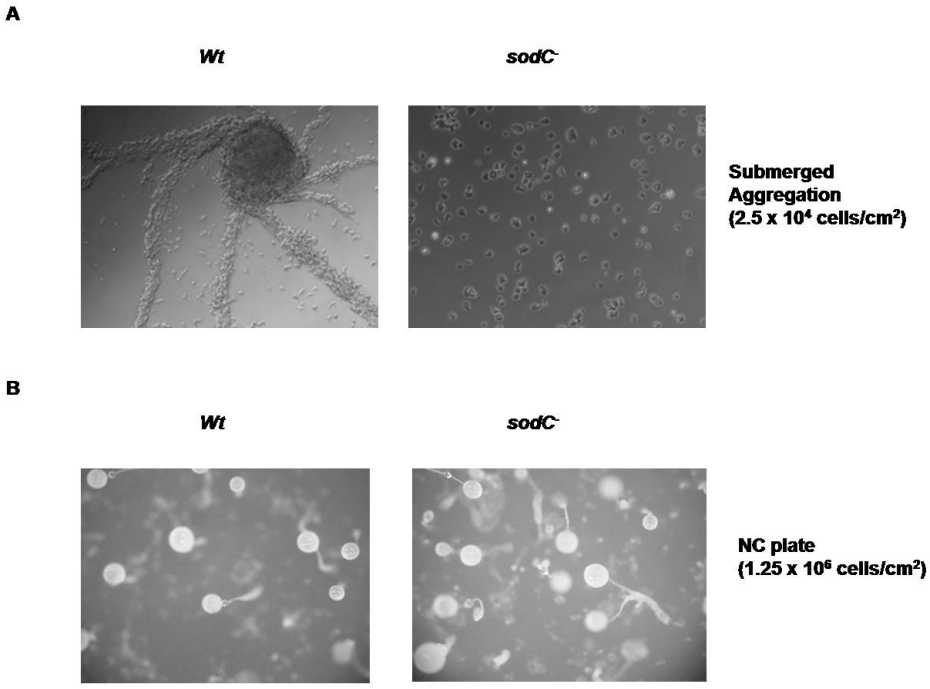

Figure 3.5 *sodC*$^-$ cells were defective in aggregation, but not development. **A.** *sodC*$^-$ cells failed to aggregate in submerged culture at low cell density (2.5 x 10^4 cells/cm^2), where wild type cells aggregate normally. **B.** *sodC*$^-$ cells displayed normal development when plated at high cell densities (1.25 x 10^6 cells/cm^2) where chemotaxis can be bypassed.

Cells lacking *SodC* displayed less polarization during the first 20 minutes under both weak and strong gradient than wild type cells. An improvement in the polarity from 0.6 to 0.3 was observed from *sodC*$^-$ cells under strong gradient during the latter 20-minute duration, whereas no such improvement was made from *sodC*$^-$ cells under weak gradient (Fig. 3.6D). *sodC*$^-$ cells displayed multiple problems in chemotaxis which can not easily be overcome by higher concentration of or longer exposure to chemoattractant cAMP.

A

Wt

0.1μM cAMP *10 μM cAMP*

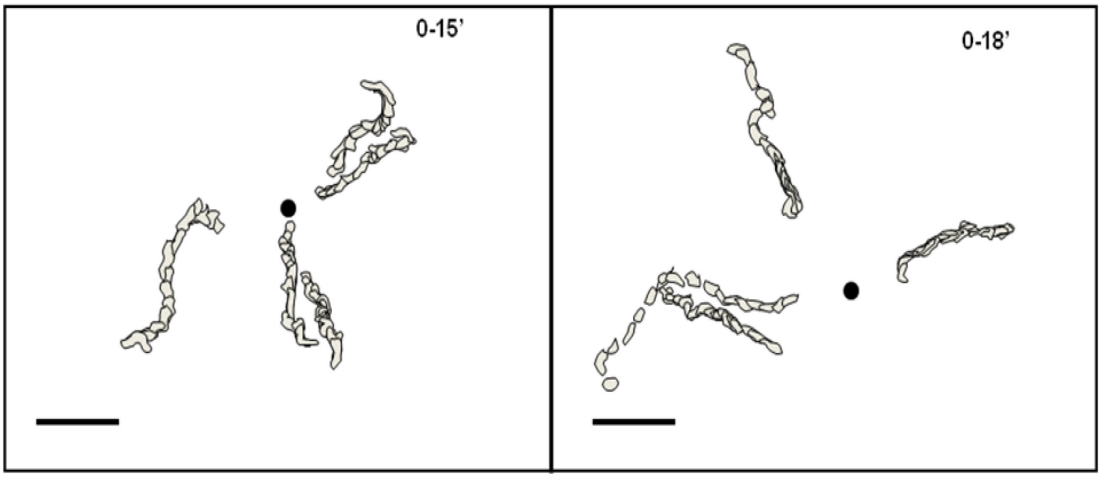

B

sodC-

0.1μM cAMP

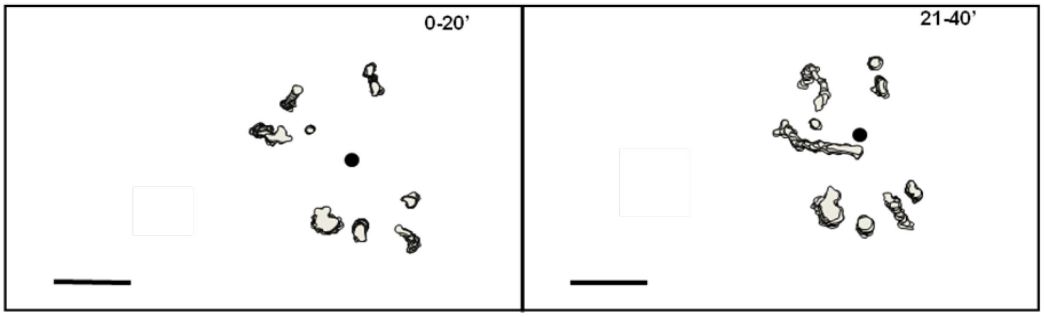

C

10 μM cAMP

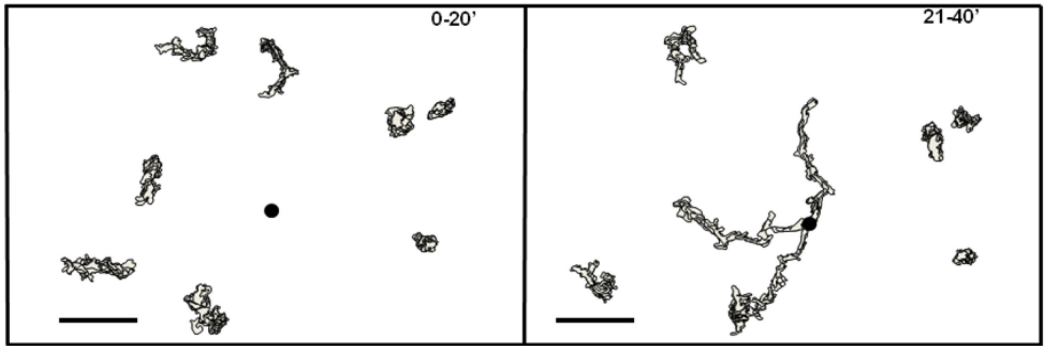

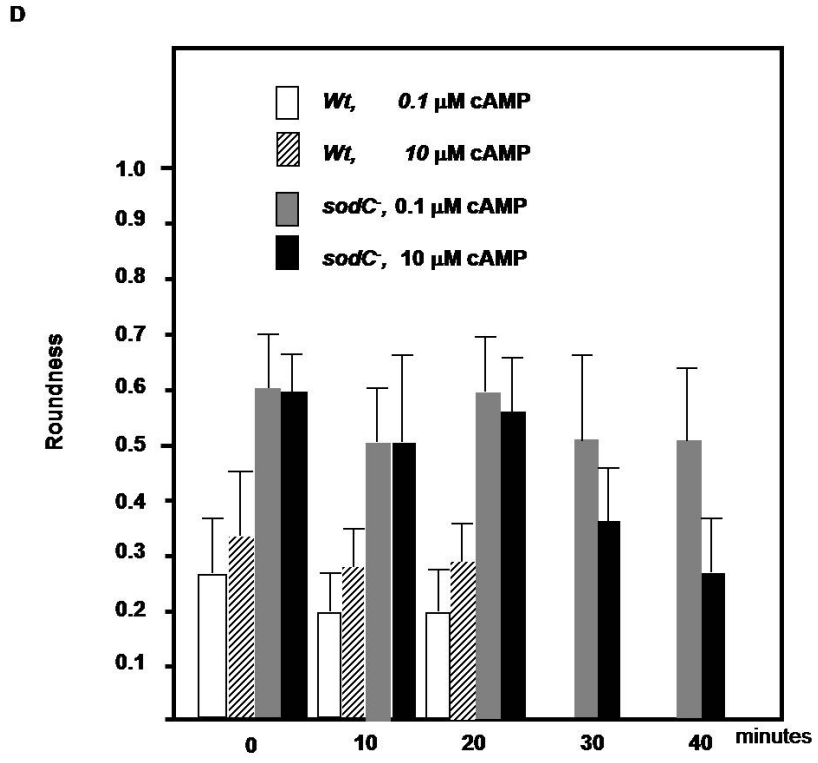

Figure 3.6 *sodC*$^-$ cells were defective in chemotaxis. **A-C.** Cells were challenged with a point source of either 0.1 μM or 10 μM cAMP. Tracing images of chemotaxing cells were arranged to demonstrate relative directional movement, cell shape, and distances traveled toward the cAMP point source (a gray circle). Superimposed tracing images were grouped as early (0-20') and late (21'-40') duration as marked. Each tracing images is at 1-minute intervals. **D.** Roundness of chemotaxing cells were summarized as defined in the materials and methods.

Table 3.1 Summary of chemotactic indices and motilities of *sodC*$^-$ cells. Mean values with standard deviations from three independent experiments were shown.

	cAMP	Response	0-20 min	21-40 min
sodC$^-$	0.1 μM	Chemotaxis Index	0.16 ± 0.36	0.31 ± 0.34
		Speed (μm/min)	1.6 ± 0.3	2.2 ± 1.2
	10 μM	Chemotaxis Index	0.00 ± 0.34	0.29 ± 0.36
		Speed (μm/min)	5.2 ± 1.3	5.7 ± 2.5
Wt	0.1 μM	Chemotaxis Index	0.82±0.10	
		Speed (μm/min)	9.2± 2.6	
	10 μM	Chemotaxis Index	0.79±0.12	
		Speed (μm/min)	9.2 ± 4.7	

3.2.5 Reintroduction of wild type SodC, not the inactive mutant SodC, partially attenuated chemotaxis defects of *sodC*$^-$ cells

A previous study showed that the substitution of the two histidine residues in the Copper binding motif of the SOD domain with arginine and glutamate were led to an effective loss of Sod activity (Wang et al., 2002). Similarly, the catalytically inactive *SodC (H245R,H247Q)* was generated and expressed in *sodC*$^-$ cells. Levels of *SodC* transcripts were compared in wild type, *sodC*$^-$ cells, *sodC*$^-$ cells expressing wild type *SodC* or *SodC(H245R,H247Q)* by RT-PCR as shown in figure 3.7A. A clear *SodC* message was detected from wild type cells, but not from *sodC*$^-$ cells. *sodC*$^-$ cells

expressing wild type *SodC* or *SodC(H245R,H247Q)* displayed a comparable level of *SodC* message, which is higher than that of the endogenous *SodC* messages.

Cells lacking *SodC* with this level of reintroduced *SodC* messages were challenged with a micropipette filled with 0.1 μM cAMP for 20 minutes. The chemotaxis index of *sodC*$^-$ cells expressing the full length *SodC* was near ~90% of the wild type level, and their speed improved to ~40% of the wild type level. In contrast, chemotaxis index of *sodC*$^-$ cells expressing SodC(H245R, H247Q) was similar to that of the parental *sodC*$^-$ cells (Fig.3.7). Although the complementation was less than complete, there was a clear improvement in chemotaxis and cell polarization by wild type SodC expression but not by the mutant one in *sodC*$^-$ cells (Table 3.2 and Fig. 3.7C).

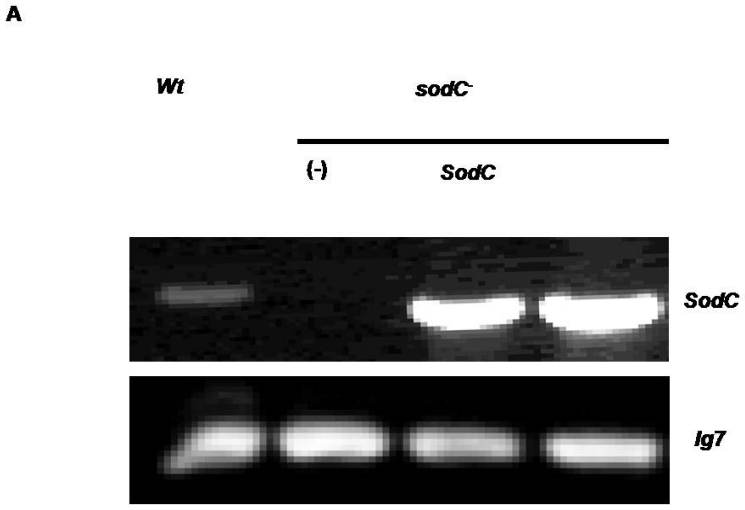

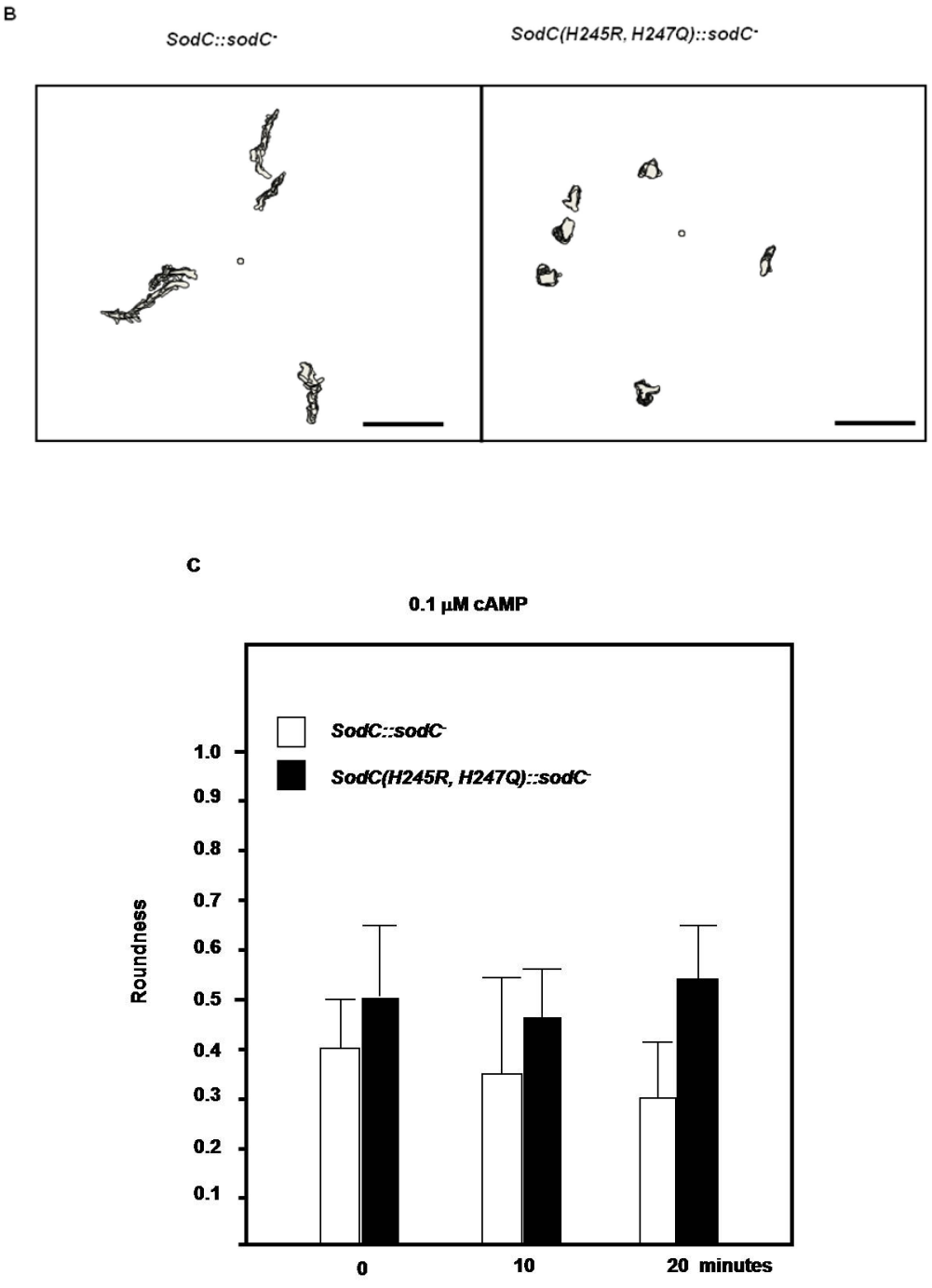

Figure 3.7 Defects in *sodC*- cells were partially rescued by SodC but not with SodC(H245R,H247Q) double point mutant. **A.** RT-PCR experiment with a primer set specific for SodC was used to detect the level of *SodC* transcript. A specific RT-PCR

product was obtained from wild type, but not from *sodC*$^-$ cells as expected. *Ig7* transcripts were used as a control. Similar levels of the transcripts were observed from *sodC*$^-$ cells expressing wild type SodC and SodC(H245R,H247Q) mutant under Actin-15 promoter. **B.** *sodC*$^-$ cells expressing wild type SodC and SodC(H245R,H247Q) mutant were challenged with a micropipette filled with 0.1 μM cAMP for 20 minutes. 20 stacks of tracing images are shown with a 100 μm scale bar. **C.** Summary of the roundness were shown.

Table 3.2 Summary of chemotactic indices and motilities of *sodC*$^-$ cells expressing either wild type *SodC* or *SodC(H245R,H247Q)* double point mutant.

0.1 μM cAMP	*SodC::sodC*$^-$	*SodC(H245R,H247Q) ::sodC*$^-$
Chemotaxis Index (Mean ± SD)	0.66 ± 0.31	0.29 ± 0.27
Speed (μm/min) (Mean ± SD)	3.5 ± 1.4	1.0 ± 0.2

3.2.6 *sodC*$^-$ cells pretreated with PI3K inhibitor LY294002 exhibited improved chemotaxis

To determine if *sodC*$^-$ cells are defective in chemotaxis mainly the result of the presence of an excessive PIP3, cells expressing PIP3 marker GFP-PHcrac were pulsed for 4 hours with 50 nM cAMP, and either left in DB buffer or treated with 15 μM or 50 μM of PI3K inhibitor LY294002 (LY) for 20 min. *sodC*$^-$ cells expressing GFP-PHcrac showed aberrant plasma membrane localization, which decreased significantly at the

plasma membrane after treatment with 15 μM or 50 μM LY294002 (Fig. 3.8A). However, LY294002 treated *sodC*$^-$ cells still displayed PIP3 enriched macropinosomes and local ruffles, indicating that PIP3 levels were attenuated but not completely depleted (Fig.3.8A).

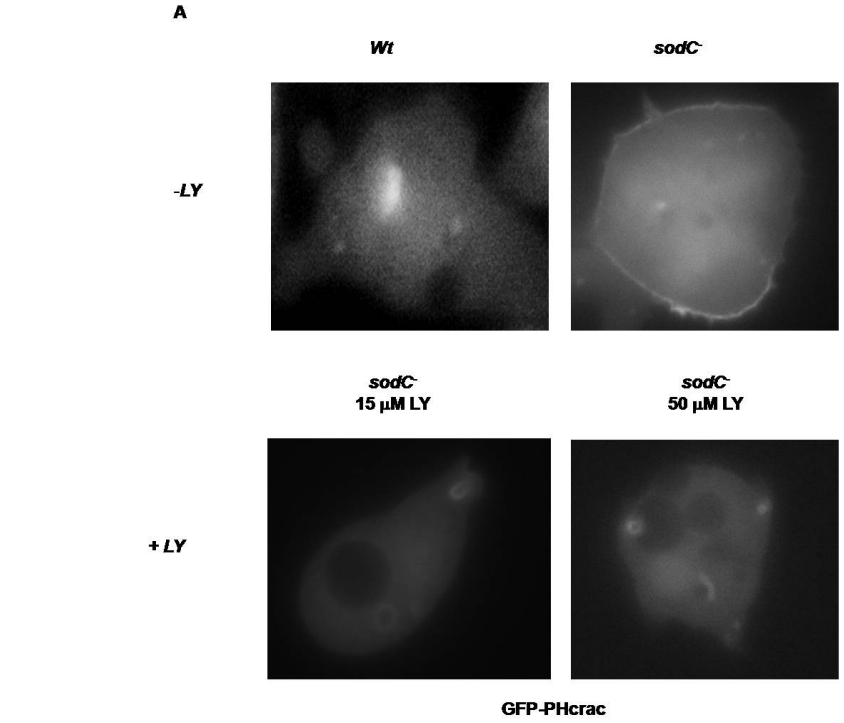

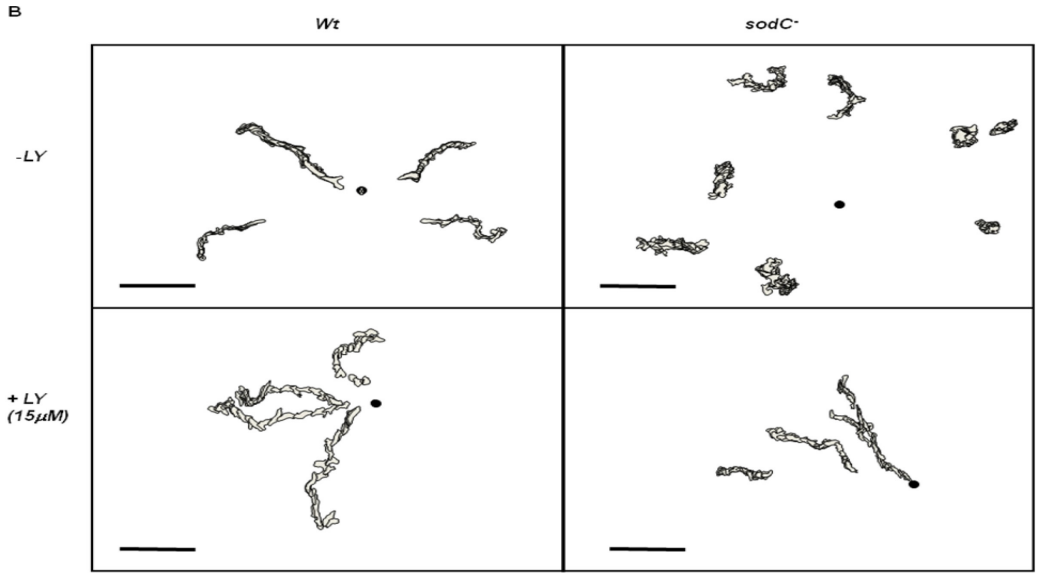

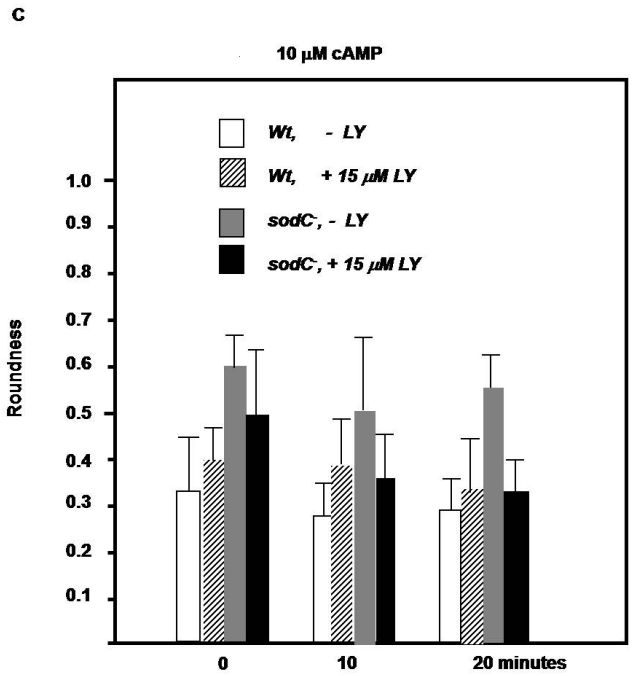

Figure 3.8 LY294002 treatment attenuated chemotaxis defects of *sodC*$^-$ cells. **A.** Cells expressing PIP3 marker GFP-PHcrac were pulsed for 4 hours with 50 nM cAMP, and either left in DB buffer or treated with 15 μM or 50 μM LY294002 (LY) for 20 minutes. GFP-PHcrac aberrantly localized at the plasma membrane of *sodC*$^-$ cells compared to wild type. Membrane localization of GFP-PHcrac in *sodC*$^-$ cells largely disappeared after LY treatment. GFP signals at the membrane of *sodC*$^-$ cells were reminiscent of fine filopodial extensions, which also disappeared after LY treatment. **B.** Wild type and *sodC*$^-$ cells were pulsed for 4 hours with 50 nM cAMP, and treated with and without 15 μM LY294002 (LY) for 20 minutes. Cells were then challenged with micropipettes filled with 10 μM cAMP for 20 minutes. Twenty stacks of cell tracing images, each of which is 1 minute apart, were shown with a 100 μm scale bar. **C.** Roundness values of the analyzed cells were shown.

Then, wild type and *sodC*$^-$ cells were incubated with 15 μM LY294002 for 20 min, and challenged with micropipette filled with 10 μM cAMP for 20 min. Wild type cells showed comparable chemotaxis indices and speeds irrespective of 15 μM LY294002 treatment (Fig. 3.8). Untreated *sodC*$^-$ cells almost completely failed to respond to micropipette filled with 10 μM cAMP (Fig. 3.8). In contrast, *sodC*$^-$ cells pretreated with LY294002, displayed near wild type level of gradient sensing, significantly improved speed of motility, and cell polarization (Table 3.3 and Fig. 3.8C). In contrast, the restoration of the speed of locomotion by LY treatment was not rescued (Table 3.3).

Table 3.3 Summary of chemotactic indices and motilities of wild type and *sodC*$^-$ cells treated with LY294002.

	Response	*Wt*	*sodC*$^-$
- LY	Chemotaxis Index (Mean ± SD)	0.79 ± 0.12	0.00 ± 0.33
	Speed (μm/min) (Mean ± SD)	9.2 ± 4.7	5.4 ± 1.3
+ 15 μM LY	Chemotaxis Index (Mean ± SD)	0.70 ± 0.19	0.80 ± 0.17
	Speed (μm/min) (Mean ± SD)	9.8 ± 1.6	6.0 ± 3.1

3.2.7 *sodC*$^-$ cells displayed aberrant PI3K regulation

Regulation of PI3K1 and PI3K2, the two major enzymes largely responsible for chemoattractant-induced PIP3 generation in *Dictyostelium,* is complex. Through a yet to be identified mechanism, cells control membrane and cytoplasmic localization of PI3K

(Funamoto et al., 2003). In addition, activation of Ras proteins leads to an enhanced PI3K activity. Subsequently, more PIP3 will accumulate, which in turn stimulate membrane localization of PI3K through a F-Actin dependent mechanism (Sasaki et al., 2004). In the absence of chemoattractant stimulation, wild type cells maintain a minor, but detectible, fraction of PI3K at the plasma membrane (Han et al., 2006; Sasaki et al., 2004).

The *sodC*$^-$ cells displayed N-PI3K1-GFP proteins localized uniformly throughout the plasma membrane, whereas wild type cells displayed a strong enrichment at the leading front (Fig. 3.9A). This was further confirmed by western blot analysis on the membranous and cytosolic fractions prepared from cells expressing equivalent amount of N-PI3K1-GFP proteins (Fig. 3.9B).

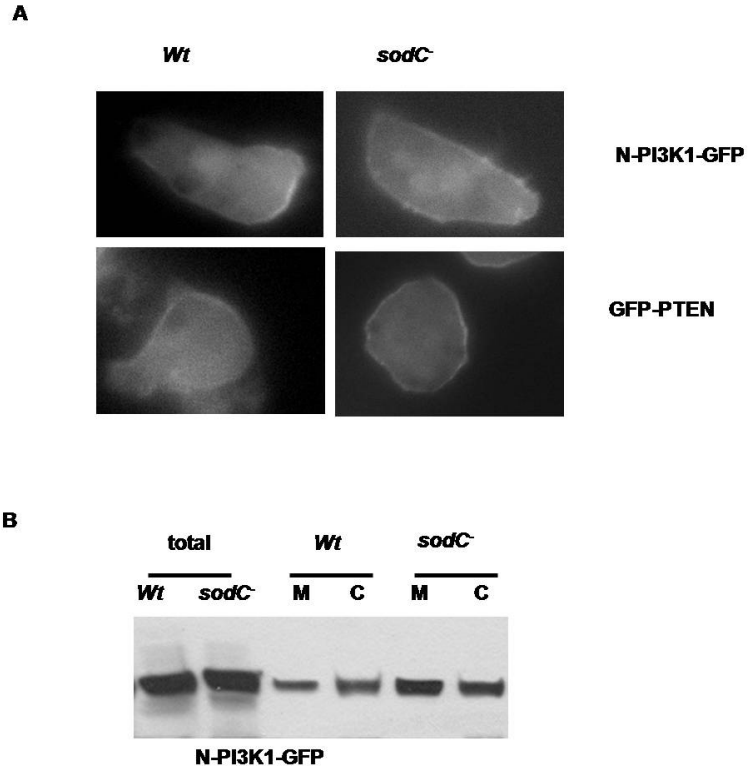

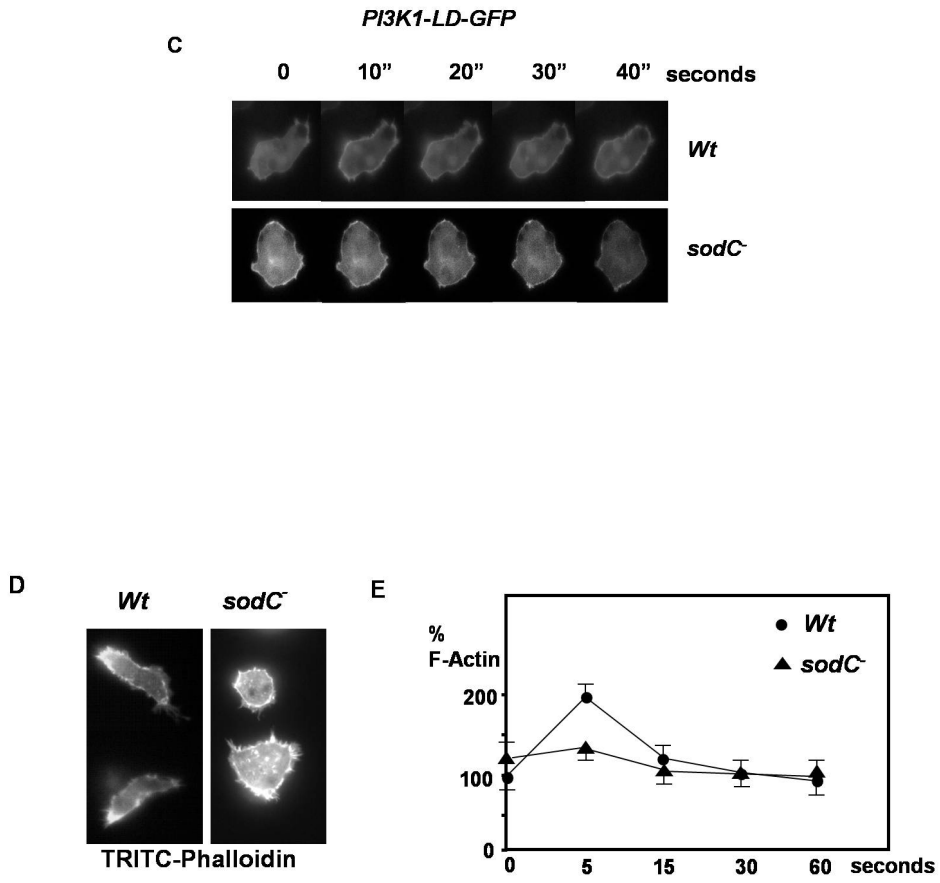

Figure 3.9 Aberrant localization of PI3K in *sodC*- cells. **A.** The membrane localization domain of PI3K1 (N-PI3K1) fused with GFP was expressed in wild type and *sodC*- cells. Aggregation competent, polarized wild type cells clearly demonstrated localized PI3K membrane translocation at the leading edge, whereas *sodC*- cells showed no PI3K polarization around the membrane. In contrast, GFP-PTEN localization was indistinguishable between wild type and *sodC*- cells. **B.** 0.01% Triton X100 fraction showed that more N-PI3K1-GFP proteins were aberrantly enriched at the membrane fraction of *sodC*- cells than that of wild type cells. **C.** Cells expressing PI3K1-LD-GFP

proteins were pulsed with 50nM cAMP for 4 hours, and stimulated with 10 μM cAMP. Membrane translocation of PI3K1-LD protein was recorded with 10 seconds of interval. Clear membrane localization of PI3K1-LD was observed from wild type cells, but no such changes were seen in *sodC*$^-$ cells. **D.** Cells were pulsed for 4 hours, fixed, and stained with TRITC-Phalloidin as described in the materials and methods. Two representative images were shown for each wild type and *sodC*$^-$ cells. Wild type cells displayed more polarized cell bodies with a leading edge enriched with F-Actin. In contrast, *sodC*$^-$ cells were much more round than the wild type and showed numerous filopodia like structures instead of a dominant pseudopodium. **E.** Pulsed cells were stimulated with 10 μM cAMP as indicated, and lysed with a F-Actin buffer containing 0.2 % of Triton X-100 and TRITC-Phalloidin, and the F-Actin levels were measured as described in the materials and methods. *sodC*$^-$ cells displayed higher basal level of F-Actin compared to that of the wild type, but no wild type like response was observed after cAMP stimulation.

Localization of the other major regulator of PIP3, PTEN, was also examined. No significant difference in the localization of GFP fused PTEN proteins was observed from wild type and *sodC*$^-$ cells (Fig. 3.9A). The aberrancy in the localization of N-PI3K1-GFP in *sodC*$^-$ cells was further highlighted when examined upon global stimulation with cAMP. Instead of a transient membrane localization observed in wild type, N-PI3K1-GFP showed membrane localization before the stimulation, which virtually did not change in response to global cAMP stimulation (Fig. 3.9C). *sodC*$^-$ cells consistently displayed less polarized cell shapes.

To examine the F-Actin organization in cAMP pulsed *sodC*$^-$ cells, cells were stained with TRITC-Phalloidin (Fig. 3.9D). While polarized wild type cells showed a dominant leading front enriched with F-Actin, *sodC*$^-$ cells exhibited numerous filopodial extensions and membrane ruffles around their more round cell bodies. When stimulated with 10 μM cAMP, wild type cells displayed a two fold increase in F-Actin level after 5 seconds of stimulation, which rapidly decreased close to the basal level. In contrast, *sodC*$^-$ cells exhibited ~20% higher basal F-Actin level compared to that of the wild type, but showed no further increase in response to cAMP stimulation (Fig. 3.9E).

3.2.8 SodC regulates Ras, an upstream regulator of PI3K

Ras is an upstream regulator of PI3K, and subject to regulation by superoxide *in vitro* (Cox and Der, 2003; Heo and Campbell, 2005; Sasaki et al., 2004). I tested if Ras is aberrantly regulated in *sodC*$^-$ cells by using GFP-RBD (Ras-Binding Domain) protein, which was previously used as an active Ras marker in *Dictyostelium* cells (Sasaki et al., 2004). Active Ras proteins in cells were indirectly visualized by monitoring GFP-RBD proteins after 4 hours of pulsing. As shown in figure 10A, wild type cells almost always showed polarized GFP-RBD localization after 4 hours of cAMP pulsing. Cells with *sodC*$^-$ background, in contrast, displayed a strikingly disorganized pattern of GFP-RBD protein (Fig. 3.10A). Furthermore, more active Ras proteins were detected from *sodC*$^-$ cells than wild type cells by GST-RBD pull-down assay (Fig. 3.10B) (Sasaki et al., 2004). In addition, when stimulated globally with 10 μM cAMP, *sodC*$^-$ cells displayed higher basal Ras proteins than wild type cells with no further increase in the active Ras

level. In contrast, wild type cells displayed the transient Ras activation as expected (Fig. 3.10C).

To further determine if the loss of SodC directly affect Ras activity or indirectly through regulating superoxide level, cells were stimulated with conditioned medium with or without a superoxide scavenger XTT. A previous study showed that conditioned medium prepared by cAMP pulsing stimulated cellular superoxide generation (Bloomfield and Pears, 2003). *sodC*$^-$ cells displayed a higher basal level of active Ras as expected, but showed a significant decrease of active Ras level upon depletion of superoxide by incubation with radical scavenger XTT (4 mM) for 10 minutes at room temperature (Fig. 3.10D). A much lower level of active endogenous Ras was observed from wild type cells, which was also susceptible to XTT treatment (Fig. 3.10D).

Next, the identity of aberrantly activated Ras species in *sodC*$^-$ cells was determined. A previous study identified that RasG is one of the major Ras proteins that regulates chemotaxis and is capable of binding to the human Raf1-RBD when activated (Sasaki et al., 2004). Consistent with this, basal activity of GFP-RasG was identified to be higher in *sodC*$^-$ cells than wild type cells (Fig. 3.10E). Also, stimulation of wild type cells with the CM showed a modest increase in the level of active GFP-RasG, which was susceptible to XTT treatment (Fig. 3.10F). In contrast, *sodC*$^-$ cells displayed higher basal level of active GFP-RasG, which was not responsive to the stimulation with the CM but susceptible to XTT treatment (Fig. 3.10F).

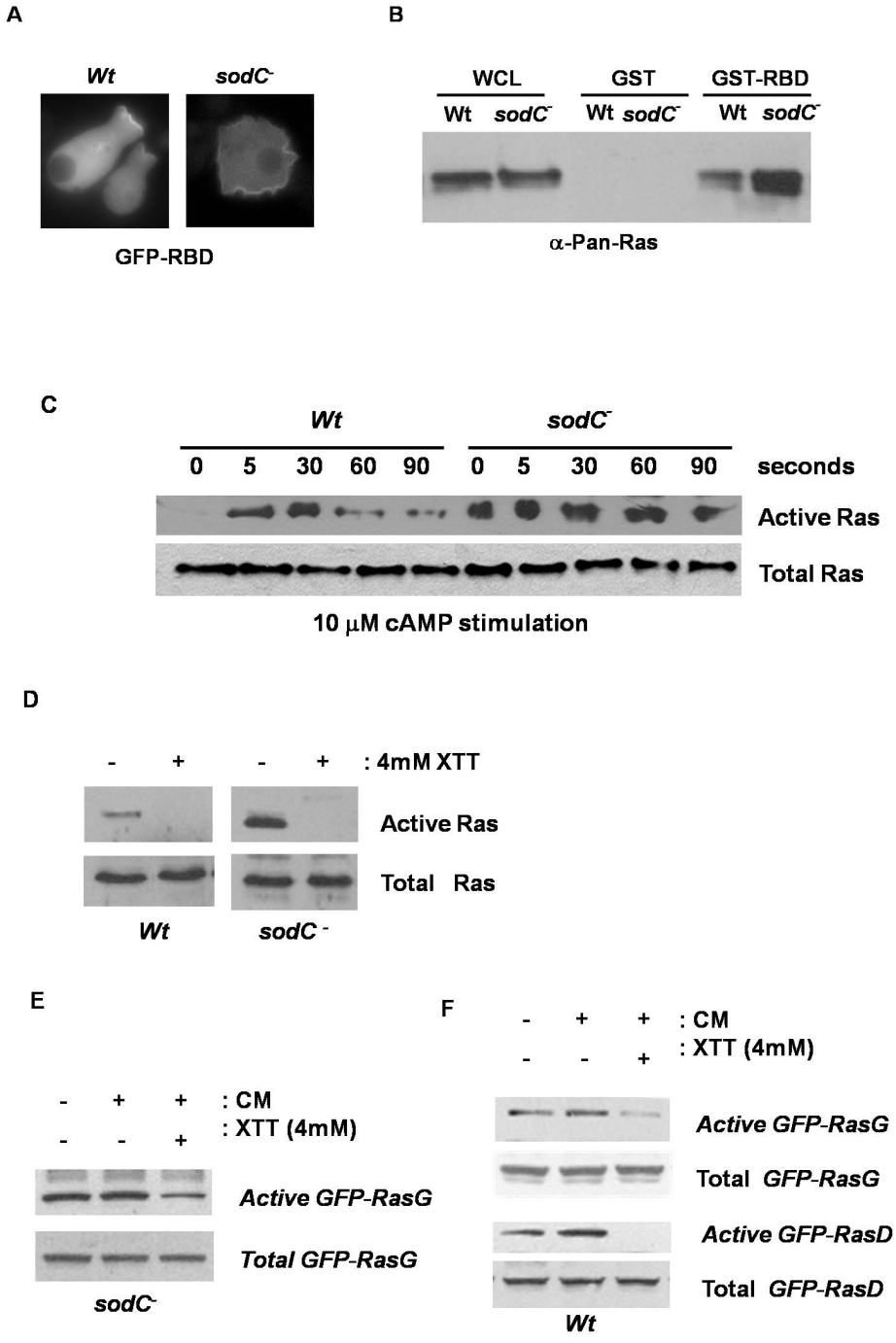

Figure 3.10 Ras proteins were not properly regulated in *sodC*$^-$ cells. **A.** Active Ras proteins were visualized by GFP-RBD signals on the plasma membrane. Wild type cells

often displayed well-organized RBD signal on one side of a cell, whereas *sodC*$^-$ exhibited broad GFP-RBD signal around cellular peripheries. Images were after 4 hours of cAMP pulsing. **B.** Significantly higher basal level of active Ras was detected from *sodC*$^-$ cells than wild type cells after 4 hours of pulsing. **C.** Cells were pulsed with 50nM cAMP for 4 hours, and then stimulated with 10 μM cAMP as indicated. Amount of total Ras proteins were first normalized by western blot using anti-Pan-Ras antibody. Active Ras proteins were determined by GST-RBD assay (Sasaki et al., 2004). **D.** Higher basal level of active Ras in *sodC*$^-$ cells was significantly decreased upon depletion of superoxide by incubation with radical scavenger XTT (4 mM) for 10 minutes at room temperature. As also shown in figure 10C, wild type cells showed lower level of active Ras. **E.** *sodC*$^-$ cells displayed higher basal level of active GFP-RasG than wild type cells. **F.** GFP-RasG was modestly activated by CM and was susceptible to XTT in wild type cells. In *sodC*$^-$ cells, GFP-RasG showed higher basal activity and was susceptible to XTT, but no further stimulation of GFP-RasG was observed with CM.

3.3 Discussion and future directions

Preliminary results suggested that SodC is a membrane protein, possibly functioning at the outer membrane by anchoring with the GPI anchor. It is intriguing to fathom the function of SodC at the outer membrane, given that the majority of the SODs identified so far are intracellular and are implicated in nullifying the radicals generated from mitochondrial oxidative respiration. Moreover, the mechanisms of superoxide radical generation in *Dictyostelium* are largely unknown, particularly at the plasma membrane. Nonetheless, it was shown that superoxide radicals can be induced by an

unknown factor which is secreted from developmentally competent cells, and superoxide radicals are necessary for proper aggregation (Bloomfield and Pears, 2003). My studies suggest the possibility of the existence of membrane bound superoxide radical generating proteins in *Dictyostelium*, such as NADPH oxidase which was shown in other organisms (Hancock et al., 2001). In such scenarios, it is possible that radicals generated at the membrane can be rapidly protonated and pass through the plasma membrane (Korshunov and Imlay, 2002) and might be responsible for the increased intracellular superoxide radical pool in the absence of SodC. Even though there is a modest increase in the total intracellular super oxide radical levels in the absence of SodC, it is possible that this increase could be at much higher levels in the immediate vicinity of the membrane than the total average number. This possibility might explain the pronounced effects of superoxide radicals penetrated into the cell on the membrane bound molecules preferentially. Also, intracellular superoxide dismutases might prevent the pleotrophic effects of penetrated radicals on the other potential targets.

As expected from the excess PIP3 levels at the membrane (Iijima and Devreotes, 2002), the *sodC*$^-$ cells were defective in performing directional motility and failed to sense the gradient and to polarize. The fact that chemotactic defects can be corrected by expressing functional superoxide dismutase, but not by mutant superoxide dismutase with no dismutation function, further support the role of SodC in conferring the chemotactic ability. Moreover, suppression of excess PIP3 levels at the membrane by a PI3 kinase pharmacological inhibitor also rescued the chemotactic defects; this result is comparable to the results from a previous study (Chen et al., 2007) . It is significant that the concentrations of the PI3K inhibitor which improved the function of *sodC*$^-$ cells did

not adversely affect the chemotactic ability of the wild type cells. These concentrations were comparable to the previous studies (Loovers et al., 2006; Takeda et al., 2007). In line with the possibility of excess PI3 kinase function in the absence of SodC, we were able to observe excess membrane localization of PI3K by both cell imaging and biochemical analysis. Although suppression of excess PIP3 levels rescued the majority of the chemotactic defects, it failed to correct the defects associated with the motility of the cells, as they exhibited poor speed after treatment with the LY294002. This observation further suggested the broader nature of defects in the absence of SodC than were caused by the excess PIP3 levels alone at the membrane and is consistent with observed excess Ras activation. This possibility might explain the inability of the LY294002 in complete rescue of *sodC*$^{-}$ chemotactic defects, as excessively activated Ras proteins are still present after LY294002 treatment. Ras molecules were shown to regulate the actin cytoskeleton not only through PIP3 pathway but also through TORC2 complex (Lee et al., 2005).

The ability of the super oxide radical scavenger XTT to suppress basal active Ras levels in wild type cells suggested the potential role of superoxide radicals in the maintenance of basal activate of Ras during random motility. Previous studies showed that excessive amounts of active RasG(G12T) levels cause multiple filopodial extensions, membrane ruffles and defective cell motility (Khosla et al., 1996; Zhang et al., 1999), and these effects were also seen in the absence of SodC. Moreover, RasG was shown to be the major species found in Ras-GTPs pulled down by the RBD used in our studies (Sasaki et al., 2004). The actin defects observed in the absence of SodC, and the ability of the superoxide radicals to activate GFP-RasG that is susceptible to XTT scavenging

activity, together with the previous studies, strongly indicate that excessively activated RasG could be one of Ras species that is causing the defective chemotaxis and excessive PIP3 levels in *sodC*$^-$ cells.

Though our studies have identified a possible role for supeoxide in Ras activation, it is not clear how superoxide is activating Ras. There could be two possible scenarios. First, superoxide might be activating Ras by directly modifying it through oxidation. It is suggested (Heo and Campbell, 2005) that the cysteine amino acid that is crucial in holding the GDP when Ras is in its inactive state could be the target for superoxide oxidation. Such oxidation might lead to the release of GDP and may give the opportunity for the GTP to replace GDP, causing Ras to become activated. Modification of protein conformation and function by the reactive lipid peroxidation product, 4-hydroxy-2-*trans*-nonenal (HNE), is also worth consideration in the above mentioned Ras activation process (Esterbauer et al., 1991). The HNE was shown to activate PI3K in oxidative stress induced neurotoxicity (Abdul and Butterfield, 2007; Dozza et al., 2004). Second, superoxide may modify Ras regulators such as GEF, GAP or Gβγ and thus indirectly cause Ras activation. Evaluation of these two possible cases will provide unprecedented knowledge in understanding the superoxide radical biological effects in many contexts. It is also important to determine the Ras species that are aberrantly activated in the absence of SodC apart from RasG.

Based on the evidence obtained, we developed a hypothetical model (Fig. 3.11) to explain the function of SodC in *Dictyostelium* chemotaxis. SodC is functioning at the outer membrane with the GPI anchor, thereby preventing the entry of the superoxide radicals through the plasma membrane. In the absence of SodC, superoxide radicals are

passing through the membrane and are causing Ras activation, which in turn activates PI3K and thus causes the elevated PIP3 generation. Higher PIP3 levels, in turn, attract the PH-domain containing proteins to the membrane, especially the proteins that regulate the F-actin dynamics such as PhdA (Chisholm and Firtel, 2004).

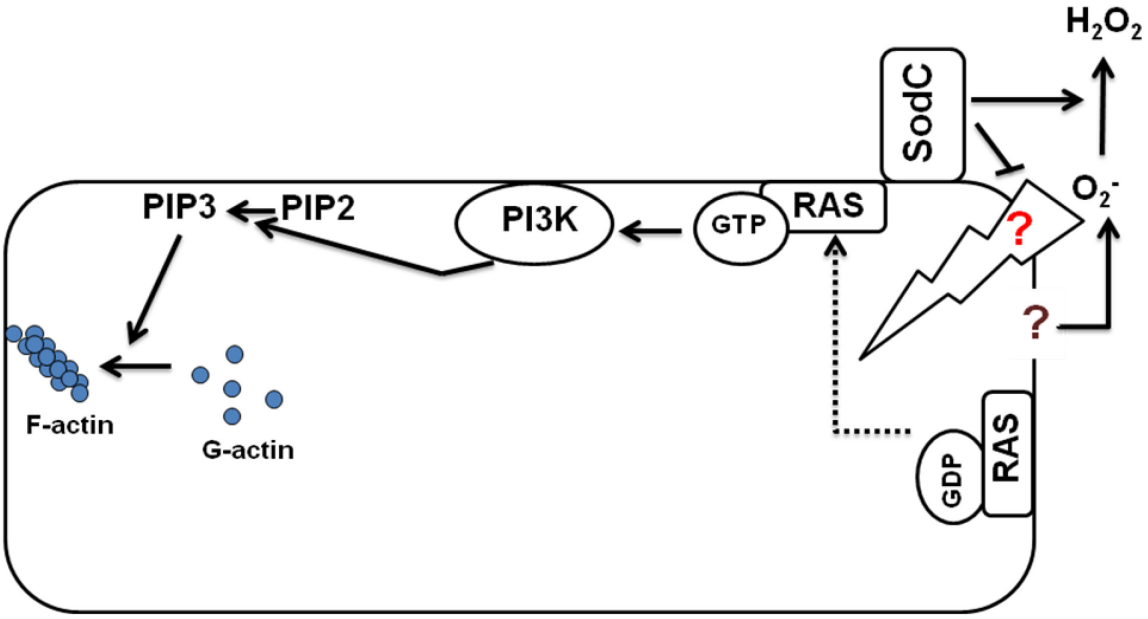

Figure 3.11 Hypothetical model explaining the function of SodC during *Dictyostelium* chemotaxis.

Given that over-expression of SOD also resulted in inhibition of aggregation (Bloomfield and Pears, 2003), and physiological levels of superoxide radicals are necessary for the maintenance of basal active Ras, the activity and/or localization of the SodC might be exquisitely controlled to fine tune Ras activation by superoxide radicals. Studies to further elaborate the dynamics of SodC in the membrane during chemotaxis might aid in understanding such exquisite controls. Understanding of the mechanisms of

superoxide generation at the plasma membrane is also important for knowing the mechanisms of superoxide mediated signaling during chemotaxis.

3.4 Significance

This work is the result of a search for regulators of cell movement using *Dictyostelium*. This study has identified a novel link between superoxide radicals and the important membrane protein Ras, which has roles in cancer and cell motility apart from other functions. Such links with further confirmatory and explanatory studies have the potential not only to appreciate the intricate complexity and elegance of regulation of biological processes, but also to develop novel and better interventions.

BIBLIOGRAHPY

Abdul, H. M. and Butterfield, D. A. (2007). Involvement of PI3K/PKG/ERK1/2 signaling pathways in cortical neurons to trigger protection by cotreatment of acetyl-L-carnitine and alpha-lipoic acid against HNE-mediated oxidative stress and neurotoxicity: implications for Alzheimer's disease. *Free Radic Biol Med* **42**, 371-84.

Alessi, D. R., Sakamoto, K. and Bayascas, J. R. (2006). LKB1-dependent signaling pathways. *Annu Rev Biochem* **75**, 137-63.

Araki, T., Tsujioka, M., Abe, T., Fukuzawa, M., Meima, M., Schaap, P., Morio, T., Urushihara, H., Katoh, M., Maeda, M. et al. (2003). A STAT-regulated, stress-induced signalling pathway in Dictyostelium. *J Cell Sci* **116**, 2907-15.

Baas, A. F., Boudeau, J., Sapkota, G. P., Smit, L., Medema, R., Morrice, N. A., Alessi, D. R. and Clevers, H. C. (2003). Activation of the tumour suppressor kinase LKB1 by the STE20-like pseudokinase STRAD. *Embo J* **22**, 3062-72.

Bloomfield, G. and Pears, C. (2003). Superoxide signalling required for multicellular development of Dictyostelium. *J Cell Sci* **116**, 3387-97.

Bokko, P. B., Francione, L., Bandala-Sanchez, E., Ahmed, A. U., Annesley, S. J., Huang, X., Khurana, T., Kimmel, A. R. and Fisher, P. R. (2007). Diverse cytopathologies in mitochondrial disease are caused by AMP-activated protein kinase signaling. *Mol Biol Cell* **18**, 1874-86.

Boudeau, J., Baas, A. F., Deak, M., Morrice, N. A., Kieloch, A., Schutkowski, M., Prescott, A. R., Clevers, H. C. and Alessi, D. R. (2003). MO25alpha/beta interact with STRADalpha/beta enhancing their ability to bind, activate and localize LKB1 in the cytoplasm. *Embo J* **22**, 5102-14.

Boudeau, J., Scott, J. W., Resta, N., Deak, M., Kieloch, A., Komander, D., Hardie, D. G., Prescott, A. R., van Aalten, D. M. and Alessi, D. R. (2004). Analysis of the LKB1-STRAD-MO25 complex. *J Cell Sci* **117**, 6365-75.

Chen, C. F. and Katz, E. R. (1998). Expression vector containing an N-terminal epitope tag for Dictyostelium discoideum. *Biotechniques* **25**, 22-4.

Chen, L., Iijima, M., Tang, M., Landree, M. A., Huang, Y. E., Xiong, Y., Iglesias, P. A. and Devreotes, P. N. (2007). PLA2 and PI3K/PTEN pathways act in parallel to mediate chemotaxis. *Dev Cell* **12**, 603-14.

Chisholm, R. L. and Firtel, R. A. (2004). Insights into morphogenesis from a simple developmental system. *Nat Rev Mol Cell Biol* **5**, 531-41.

Choi, H. S., Cha, Y. N. and Kim, C. (2006). Taurine chloramine inhibits PMA-stimulated superoxide production in human neutrophils perhaps by inhibiting phosphorylation and translocation of p47(phox). *Int Immunopharmacol* **6**, 1431-40.

Choi, S. L., Kim, S. J., Lee, K. T., Kim, J., Mu, J., Birnbaum, M. J., Soo Kim, S. and Ha, J. (2001). The regulation of AMP-activated protein kinase by H(2)O(2). *Biochem Biophys Res Commun* **287**, 92-7.

Cox, A. D. and Der, C. J. (2003). The dark side of Ras: regulation of apoptosis. *Oncogene* **22**, 8999-9006.

Dozza, B., Smith, M. A., Perry, G., Tabaton, M. and Strocchi, P. (2004). Regulation of glycogen synthase kinase-3beta by products of lipid peroxidation in human neuroblastoma cells. *J Neurochem* **89**, 1224-32.

Esterbauer, H., Schaur, R. J. and Zollner, H. (1991). Chemistry and biochemistry of 4-hydroxynonenal, malonaldehyde and related aldehydes. *Free Radic Biol Med* **11**, 81-128.

Faix, J., Gerisch, G. and Noegel, A. A. (1992). Overexpression of the csA cell adhesion molecule under its own cAMP-regulated promoter impairs morphogenesis in Dictyostelium. *J Cell Sci* **102 (Pt 2)**, 203-14.

Fogarty, S. and Hardie, D. G. (2009). C-terminal phosphorylation of LKB1 is not required for regulation of AMP-activated protein kinase, BRSK1, BRSK2, or cell cycle arrest. *J Biol Chem* **284**, 77-84.

Fosnaugh, K. L. and Loomis, W. F. (1993). Enhancer regions responsible for temporal and cell-type-specific expression of a spore coat gene in Dictyostelium. *Dev Biol* **157**, 38-48.

Funamoto, S., Meili, R., Lee, S., Parry, L. and Firtel, R. A. (2002). Spatial and temporal regulation of 3-phosphoinositides by PI 3-kinase and PTEN mediates chemotaxis. *Cell* **109**, 611-23.

Gamper, M., Kim, E., Howard, P. K., Ma, H., Hunter, T. and Firtel, R. A. (1999). Regulation of Dictyostelium protein-tyrosine phosphatase-3 (PTP3) through osmotic shock and stress stimulation and identification of pp130 as a PTP3 substrate. *J Biol Chem* **274**, 12129-38.

Ginsburg, G. T. and Kimmel, A. R. (1997). Autonomous and nonautonomous regulation of axis formation by antagonistic signaling via 7-span cAMP receptors and GSK3 in Dictyostelium. *Genes Dev* **11**, 2112-23.

Han, J. W., Leeper, L., Rivero, F. and Chung, C. Y. (2006). Role of RacC for the regulation of WASP and phosphatidylinositol 3-kinase during chemotaxis of Dictyostelium. *J Biol Chem* **281**, 35224-34.

Hancock, J. T., Desikan, R. and Neill, S. J. (2001). Role of reactive oxygen species in cell signalling pathways. *Biochem Soc Trans* **29**, 345-50.

Harwood, A. J., Plyte, S. E., Woodgett, J., Strutt, H. and Kay, R. R. (1995). Glycogen synthase kinase 3 regulates cell fate in Dictyostelium. *Cell* **80**, 139-48.

Heo, J. and Campbell, S. L. (2005). Superoxide anion radical modulates the activity of Ras and Ras-related GTPases by a radical-based mechanism similar to that of nitric oxide. *J Biol Chem* **280**, 12438-45.

Huang, Y. E., Iijima, M., Parent, C. A., Funamoto, S., Firtel, R. A. and Devreotes, P. (2003). Receptor-mediated regulation of PI3Ks confines PI(3,4,5)P3 to the leading edge of chemotaxing cells. *Mol Biol Cell* **14**, 1913-22.

Iijima, M. and Devreotes, P. (2002). Tumor suppressor PTEN mediates sensing of chemoattractant gradients. *Cell* **109**, 599-610.

Iranfar, N., Fuller, D. and Loomis, W. F. (2003). Genome-wide expression analyses of gene regulation during early development of Dictyostelium discoideum. *Eukaryot Cell* **2**, 664-70.

Jin, T., Soede, R. D., Liu, J., Kimmel, A. R., Devreotes, P. N. and Schaap, P. (1998). Temperature-sensitive Gbeta mutants discriminate between G protein-dependent and -independent signaling mediated by serpentine receptors. *Embo J* **17**, 5076-84.

Kawata, T., Nakagawa, M., Shimada, N., Fujii, S. and Oohata, A. A. (2004). A gene encoding, prespore-cell-inducing factor in Dictyostelium discoideum. *Dev Growth Differ* **46**, 383-92.

Khosla, M., Spiegelman, G. B. and Weeks, G. (1996). Overexpression of an activated rasG gene during growth blocks the initiation of Dictyostelium development. *Mol Cell Biol* **16**, 4156-62.

Kim, L., Harwood, A. and Kimmel, A. R. (2002). Receptor-dependent and tyrosine phosphatase-mediated inhibition of GSK3 regulates cell fate choice. *Dev Cell* **3**, 523-32.

Kim, L., Liu, J. and Kimmel, A. R. (1999). The novel tyrosine kinase ZAK1 activates GSK3 to direct cell fate specification. *Cell* **99**, 399-408.

Korshunov, S. S. and Imlay, J. A. (2002). A potential role for periplasmic superoxide dismutase in blocking the penetration of external superoxide into the cytosol of Gram-negative bacteria. *Mol Microbiol* **43**, 95-106.

Kumagai, A., Hadwiger, J. A., Pupillo, M. and Firtel, R. A. (1991). Molecular genetic analysis of two G alpha protein subunits in Dictyostelium. *J Biol Chem* **266**, 1220-8.

Lee, S., Comer, F. I., Sasaki, A., McLeod, I. X., Duong, Y., Okumura, K., Yates, J. R., 3rd, Parent, C. A. and Firtel, R. A. (2005). TOR complex 2 integrates cell movement during chemotaxis and signal relay in Dictyostelium. *Mol Biol Cell* **16**, 4572-83.

Lilly, P., Wu, L., Welker, D. L. and Devreotes, P. N. (1993). A G-protein beta-subunit is essential for Dictyostelium development. *Genes Dev* **7**, 986-95.

Lizcano, J. M., Goransson, O., Toth, R., Deak, M., Morrice, N. A., Boudeau, J., Hawley, S. A., Udd, L., Makela, T. P., Hardie, D. G. et al. (2004). LKB1 is a master kinase that activates 13 kinases of the AMPK subfamily, including MARK/PAR-1. *Embo J* **23**, 833-43.

Loovers, H. M., Postma, M., Keizer-Gunnink, I., Huang, Y. E., Devreotes, P. N. and van Haastert, P. J. (2006). Distinct roles of PI(3,4,5)P3 during chemoattractant signaling in Dictyostelium: a quantitative in vivo analysis by inhibition of PI3-kinase. *Mol Biol Cell* **17**, 1503-13.

Marignani, P. A. (2005). LKB1, the multitasking tumour suppressor kinase. *J Clin Pathol* **58**, 15-9.

Martens, H., Novotny, J., Oberstrass, J., Steck, T. L., Postlethwait, P. and Nellen, W. (2002). RNAi in Dictyostelium: the role of RNA-directed RNA polymerases and double-stranded RNase. *Mol Biol Cell* **13**, 445-53.

Merlot, S. and Firtel, R. A. (2003). Leading the way: Directional sensing through phosphatidylinositol 3-kinase and other signaling pathways. *J Cell Sci* **116**, 3471-8.

Ossipova, O., Bardeesy, N., DePinho, R. A. and Green, J. B. (2003). LKB1 (XEEK1) regulates Wnt signalling in vertebrate development. *Nat Cell Biol* **5**, 889-94.

Ott, A., Oehme, F., Keller, H. and Schuster, S. C. (2000). Osmotic stress response in Dictyostelium is mediated by cAMP. *Embo J* **19**, 5782-92.

Oyama, M. (1996). cGMP accumulation induced by hypertonic stress in Dictyostelium discoideum. *J Biol Chem* **271**, 5574-9.

Parent, C. A., Blacklock, B. J., Froehlich, W. M., Murphy, D. B. and Devreotes, P. N. (1998). G protein signaling events are activated at the leading edge of chemotactic cells. *Cell* **95**, 81-91.

Plyte, S. E., O'Donovan, E., Woodgett, J. R. and Harwood, A. J. (1999). Glycogen synthase kinase-3 (GSK-3) is regulated during Dictyostelium development via the serpentine receptor cAR3. *Development* **126**, 325-33.

Powell-Coffman, J. A. and Firtel, R. A. (1994). Characterization of a novel Dictyostelium discoideum prespore-specific gene, PspB, reveals conserved regulatory sequences. *Development* **120**, 1601-11.

Powell-Coffman, J. A., Schnitzler, G. R. and Firtel, R. A. (1994). A GBF-binding site and a novel AT element define the minimal sequences sufficient to direct prespore-specific expression in Dictyostelium discoideum. *Mol Cell Biol* **14**, 5840-9.

Qiu, W., Schonleben, F., Thaker, H. M., Goggins, M. and Su, G. H. (2006). A novel mutation of STK11/LKB1 gene leads to the loss of cell growth inhibition in head and neck squamous cell carcinoma. *Oncogene* **25**, 2937-42.

Sapkota, G. P., Kieloch, A., Lizcano, J. M., Lain, S., Arthur, J. S., Williams, M. R., Morrice, N., Deak, M. and Alessi, D. R. (2001). Phosphorylation of the protein kinase mutated in Peutz-Jeghers cancer syndrome, LKB1/STK11, at Ser431 by p90(RSK) and cAMP-dependent protein kinase, but not its farnesylation at Cys(433), is essential for LKB1 to suppress cell vrowth. *J Biol Chem* **276**, 19469-82.

Sasaki, A. T., Chun, C., Takeda, K. and Firtel, R. A. (2004). Localized Ras signaling at the leading edge regulates PI3K, cell polarity, and directional cell movement. *J Cell Biol* **167**, 505-18.

Sasaki, A. T., Janetopoulos, C., Lee, S., Charest, P. G., Takeda, K., Sundheimer, L. W., Meili, R., Devreotes, P. N. and Firtel, R. A. (2007). G protein-independent Ras/PI3K/F-actin circuit regulates basic cell motility. *J Cell Biol* **178**, 185-91.

Shaw, R. J., Kosmatka, M., Bardeesy, N., Hurley, R. L., Witters, L. A., DePinho, R. A. and Cantley, L. C. (2004). The tumor suppressor LKB1 kinase directly activates AMP-activated kinase and regulates apoptosis in response to energy stress. *Proc Natl Acad Sci U S A* **101**, 3329-35.

Strmecki, L., Bloomfield, G., Araki, T., Dalton, E., Skelton, J., Schilde, C., Harwood, A., Williams, J. G., Ivens, A. and Pears, C. (2007). Proteomic and microarray analyses of the Dictyostelium Zak1-GSK-3 signaling pathway reveal a role in early development. *Eukaryot Cell* **6**, 245-52.

Sussman, M. (1987). Cultivation and synchronous morphogenesis of Dictyostelium under controlled experimental conditions. *Methods Cell Biol* **28**, 9-29.

Takeda, K., Saito, T., Tanaka, T., Morio, T., Maeda, M., Tanaka, Y. and Ochiai, H. (2003). A novel gene trap method using terminator-REMI and 3' rapid amplification of cDNA ends (RACE) in Dictyostelium. *Gene* **312**, 321-33.

Takeda, K., Sasaki, A. T., Ha, H., Seung, H. A. and Firtel, R. A. (2007). Role of phosphatidylinositol 3-kinases in chemotaxis in Dictyostelium. *J Biol Chem* **282**, 11874-84.

Tsuji, A., Akaza, Y., Nakamura, S., Kodaira, K. and Yasukawa, H. (2003). Multinucleation of the sodC-deficient Dictyostelium discoideum. *Biol Pharm Bull* **26**, 1174-7.

Van Driessche, N., Shaw, C., Katoh, M., Morio, T., Sucgang, R., Ibarra, M., Kuwayama, H., Saito, T., Urushihara, H., Maeda, M. et al. (2002). A transcriptional profile of multicellular development in Dictyostelium discoideum. *Development* **129**, 1543-52.

Veeranki, S., Kim, B. and Kim, L. (2008). The GPI-anchored superoxide dismutase SodC is essential for regulating basal Ras activity and for chemotaxis of Dictyostelium discoideum. *J Cell Sci* **121**, 3099-108.

Wang, J., Xu, G., Gonzales, V., Coonfield, M., Fromholt, D., Copeland, N. G., Jenkins, N. A. and Borchelt, D. R. (2002). Fibrillar inclusions and motor neuron degeneration in transgenic mice expressing superoxide dismutase 1 with a disrupted copper-binding site. *Neurobiol Dis* **10**, 128-38.

Watts, J. L., Morton, D. G., Bestman, J. and Kemphues, K. J. (2000). The C. elegans par-4 gene encodes a putative serine-threonine kinase required for establishing embryonic asymmetry. *Development* **127**, 1467-75.

Woods, A., Johnstone, S. R., Dickerson, K., Leiper, F. C., Fryer, L. G., Neumann, D., Schlattner, U., Wallimann, T., Carlson, M. and Carling, D. (2003). LKB1 is the upstream kinase in the AMP-activated protein kinase cascade. *Curr Biol* **13**, 2004-8.

Ylikorkala, A., Rossi, D. J., Korsisaari, N., Luukko, K., Alitalo, K., Henkemeyer, M. and Makela, T. P. (2001). Vascular abnormalities and deregulation of VEGF in Lkb1-deficient mice. *Science* **293**, 1323-6.

Zhang, T., Rebstein, P. J., Khosla, M., Cardelli, J., Buczynski, G., Bush, J., Spiegelman, G. B. and Weeks, G. (1999). A mutation that separates the RasG signals that regulate development and cytoskeletal function in Dictyostelium. *Exp Cell Res* **247**, 356-66.

APPENDIX

Putative LKB1 promoter

Upstream region to LKB1 start codon (2Kb) was shown. CA rich elements necessary for prespore specific expression were shown in bold. The underlined elements represent CA elements in the opposite strand.

GGATTTAGCTGCTTATGGAATTGGTGTAAGAGATTGTATTGGTAAATCAATTGCCAAATC
TGAATTATTTACAATTTTAGCAACTTTAATTAATCGTTATGAATTTATTAATCCAGGAAC
TAATGGATTTGGAAGTTATAAAATTGGCCTTTCATGTCCTGATAATTTTATATTAATTAA
AAAAAGAAATAATAAAAATTAAAAAAAAAAAAAAAATAAGATAAATAAAAAAATCAATCTT
AATTTAACTTTATAAGTCATGTTTTATTTTTTAAAAAAAGTTAAATTTAAAAATAATTTT
AAAAAAATTTTACATTAATACTATAATATTATTATTTTTTTTTTTTTTTTTTTTTTTTTT
TTTTTCCACCACAAAGTTTTAAAAAAATAAAATAAAAATAAATAAAATAATATTAAATGA
TAATAGTATAAAAATAAAAAAAAAAAGAAGTCCAATGAAAAAAAAAATATCTAAACCCAC
TTTTTTTATTTTTTTTTTTTTTTTTTGAAATTTCGTGTGGTTTATGACAATGCTACAAAAA
ATAAACCAATAATAATTTAAAAGATAGATGATAAAATATCAATAATTTTTAAAGGAAAAA
AAAAAAAAAATATAATAATTAATATGTATATAATTTTAAAATAAAATTATTTTAAAATTA
TTTTAAAATTATTTTAAAATTATTTTATTTGAAAATAAAAAAATAATTGAAATAGTAAAA
TTTAATGGCATTAATAATTTTTTATTAATATTGCAAATTCAACTTTTTACAATAAACATT
TCAAATATATTTTCTAAACATAAAAATTTTATATATGTGTATATATGGAAAAAAAAAAAA
TAAAAAATAAAAAATAAAAAAAAAAATAACAAAAAAAAATAAAAAAAAAATAATAATAAAAA
TTATTCTTTTGCGAGATCGAATCGCGACCAGGGTCCGAATGAAATTTAAAAAAAAATAAA
GAAAAAAAAAAAAAAAAAAGAAAAAAAAATTTAAAAAAATAGTTTTGTTTTTTTTTTATT
TTTTAAATTGACACTTAAAAAAAAAGTTTTTTTTTTTTTTTTTTTTTTTTTTTTTTTTT
TTTTTTTTATTATCTAGACTTCTTTTTGTTTCCACATAAAATAATAATCAAAAAAAAAAA
ACAAAAAAAAAAAAAACAAAAAAAAAAAATAAAAAATAAAAAATAAAAAAATAATAATAAA
ACAAACAAAAAAAAAAAAAAAAAAATAAAATCATTACCACCCCCTTTGTTTGAATATAAT
TTAAATTTCACCAACAACAAAAAAAATTCCACCAAACCCC**CACACA**CCACCATTCTTCTT
TATATAAATAAATAAATAAATATATGTGTTTACTT**GTGTGTG**AG**GTGTGTG**TATAATTTG
ATAAAATAAAATTAAATTAAATAATAATTATAATAAAAATAAAAATAATAATAACAGTTT
GAAAAAAAAAAAAAAAAAAAAAAAAAAAAAAAAAAAAAAAAAAAAAAAAAAAAAAAAAA
AAAAAAAAAAAAAAAAAAAAATTCTTTTGTTTTGAAAAAAAAAAAAAAAATAAAAAAAAAA
AAAAAAAAAAATGCGTCCGTTAAAAAATAAAACAATTATATAACATCAGCTAAAAACCTA
TTAAAAATAATTATTATTGTTTATTATTATTATTTTTTTTTTTTTAATTGGAAATTTTAT
TTTTATTTTTATTTTTTTTTTTTTTATATTTAGATACCACATTATAATTTTAATACACA
AAAAAAAAAGAAAACTAATTCAGTTAAACCCAGTTTCAACCCCCTTTCACTTCAACTCAA
AT**CACACA**AAAAAAAAAAAACAAAAAAAAAAACAAACACAAACACAAAAAAAAAAGAGAG
AGAAATTTATATAGCAATATTTTATAATTTAATAATAATAATAATAAGTTTATAAATGGA
AGTTGAACAACAACCATCATATAC atggaagttgaacaacaaccatcatatacatcgaat
M E V E Q Q P S Y T S N

VITA

SUDHAKAR VEERANKI

1995-2000	B.V.Sc & A.H College of veterinary sciences Tirupati India
2000-2003	M.V.Sc Animal Genetics College of veterinary sciences Hyderabad India
2003-2004	Research assistant CDFD Hyderabad India
2004-2005	Veterinary assistant surgeon Krishna dt. Animal husbandry AP, India
2005-present	Doctoral candidate Biology Florida International University Miami, FL, USA

PUBLICATIONS AND PRESENTATIONS

Lee, N. S., Veeranki, S., Kim, B. and Kim, L. (2008). The function of PP2A/B56 in non-metazoan multicellular development. *Differentiation* **76**, 1104-10.

Rodriguez, M., Kim, B., Lee, N. S., Veeranki, S. and Kim, L. (2008). MPL1, a novel phosphatase with leucine-rich repeats, is essential for proper ERK2 phosphorylation and cell motility. *Eukaryot Cell* **7**, 958-66.

Veeranki, S., Kim, B. and Kim, L. (2008). The GPI-anchored superoxide dismutase SodC is essential for regulating basal Ras activity and for chemotaxis of Dictyostelium discoideum. *J Cell Sci* **121**, 3099-108.

S. Veeranki, B. Kim, and L. Kim. Siren1, the GPI-anchored Superoxide Desmutase inhibits PIP3 accumulation by suppressing PI3K membrane targeting. 'Biology symposium 2006', FIU, Miami, Florida, USA.

S. Veeranki, B. Kim, and L. Kim. Siren1 Regulates Cellular Navigation in Dictyostelium discoideum. Biomedical and comparative immunology symposium 2006', FIU, Miami, Florida, USA.

M. Rodriguez, N. Lee, S. Veeranki, B. Kim, and L. Kim. Dictyostelium B56 Is Essential for Both Differentiation and Cell Migration. Poster No: B571, The American society for Cell Biology 48th annual meeting, Dec 13-17 2008, San Francisco, California, USA.

S. Veeranki, B. Kim, and L. Kim. The function of SodC/ROS in PI3K signaling. Poster number: 321 Keystone Symposia: PI 3-Kinase Signaling in Disease (Z3), April 22 - April 27, 2009, Resort at Squaw Creek, Olympic Valley, CA, USA.

AWARDS

Presidential Fellow FIU, 2005-2008

Dissertation Year Fellowship FIU, 2009 summer-present

Second prize ($400) in GSA scholarly forum oral competition, FIU 2009

Travel grants:	GSA, FIU 2009	$450
	Biology Department, FIU 2009	$200
	College of Arts and Sciences, FIU	$200

HONORS

Nominated for **Phi-Kappa-Phi** honor society.

Nominated for **Golden Key International** honor society.

Nominated for **Delta Epsilon Iota** Academic honor society.